PHILOSOPHICAL TRANSACTIONS OF THE ROYAL SOCIETY A MATHEMATICAL, PHYSICAL & ENGINEERING SCIENCES

Isotopic and Chemical Effects Produced in a Continuously Differentiating Convecting Earth Mantle

C. J. Allegre, O. Brevart, B. Dupre and J.-F. Minster

Phil. Trans. R. Soc. Lond. A 1980 **297**, 447-477
doi: 10.1098/rsta.1980.0225

Phil. Trans. R. Soc. Lond. A **297**, 447–477 (1980)
Printed in Great Britain

Isotopic and chemical effects produced in a continuously differentiating convecting Earth mantle

By C. J. Allègre, O. Brévart, B. Dupré and J.-F. Minster
Laboratoire de Géochimie et Cosmochimie (*LA* 196), *Institut de Physique du Globe et Département des Sciences de la Terre, Universités de Paris* 6 *et* 7, 4 *Place Jussieu*, 75230 *Paris Cedex* 05, *France*

Trace element variations have established the present concept of chemical heterogeneity of the Earth's mantle. A continuous range of variations is observed for the mantle source of basalts, from mantle depleted in incompatible trace elements to mantle enriched in such elements, in particular light rare earth elements. This heterogeneity is supported by the study of orogenic lherzolites and ultramafic nodules from volcanoes and kimberlite pipes. Radiogenic isotopes of Sr, Pb and Nd confirm this heterogeneity and show that it results from ancient chemical fractionations. This trace element and radiogenic isotope heterogeneity is identifiable in the Precambrian mantle. Pb isotopes are the clearest tracers of this past heterogeneity.

Correlations are observed between variations in incompatible element ratios, radiogenic isotope ratios and radiogenic isotope and trace element ratios. These correlations define large domains (source of alkali basalts, source of mid-oceanic ridge basalts) and more restricted domains (e.g. the Canary Islands). Thus, they show that the mantle is heterogeneous on very large scales (ocean scales) as well as in more limited areas. Radiogenic data on ultramafic nodules also show that these mantle materials have isotopic heterogeneities at the mineral scale. These data also allow an estimation of the time scale of creation of these heterogeneities: they are of the order of some 10^9 years ($= 1$ Ga).

The mechanisms involved in the chemical evolution of the mantle are discussed. Heterogeneity is created by chemical fractionation during petrogenetic processes; essentially oceanic lithosphere formation, storage into the continental crust and also recycling of sediments during lithospheric plate subduction. This heterogeneity tends to be erased in the mantle by convection and diffusion. The former efficiently mixes the mantle at large scales. The latter is very inefficient in solid mantle conditions, but can homogenize the radiogenic isotopes during partial melting. All these processes have been continuously active through geological time. A mathematical model is proposed which describes the chemical evolution of a continuously differentiating convecting mantle. The correlations, and in particular mantle isochrons, appear as artefacts without time significance. Evolution of both trace element ratios and isotopic compositions can be described simultaneously if isotopic homogenization is easier than chemical mixing. Variations of lead isotopes tend to indicate an ancient (initial) heterogeneity of the mantle which can be possibly attributed to loss of lead from mantle to core. The rate of chemical fractionation of the mantle cannot have been constant with time but was faster during the Archaean than at present.

Introduction

Gast *et al.* (1964) have shown that the distribution of the radiogenic isotopes of strontium and lead is not homogeneous in the Earth's mantle. This also implies that the trace elements Rb, Sr, U, Th and Pb are not uniformly distributed. Since then, the chemical heterogeneity of the mantle has become increasingly well documented: see, for example, the reviews by Tatsumoto (1978) for Pb; Hofmann & Hart (1978) for Sr; and Allègre *et al.* (1979*a*) for Nd. There are currently two popular interpretations of these observations.

1. *The two-reservoir model.* This model considers that the Earth's mantle is composed of two reservoirs. One is the source of the mid-oceanic ridge basalts (m.o.r.b.), the second is that of oceanic island basalts, and is often called the 'hot-spot' reservoir. In some instances, as along the Reykjanes Ridge, these two reservoirs, or their basaltic products, appear to be mixed (Hart *et al.* 1973; Sun *et al.* 1975; White & Schilling 1978).

2. *The mantle isochron model.* Correlations are observed between the lead isotopic ratios ($^{206}Pb/^{204}Pb$–$^{207}Pb/^{204}Pb$) or ($^{206}Pb/^{204}Pb$–$^{208}Pb/^{204}Pb$); similarly the variations of the isotopic ratios $^{87}Sr/^{86}Sr$ or $^{143}Nd/^{144}Nd$ are correlated with variations in the parent/daughter element ratios Rb/Sr and Sm/Nd. These correlations, though imperfect, have been interpreted as isochrons with age significance (Tatsumoto 1966; Sun & Hanson 1975*a*; Brooks & Hart 1978; Carlson *et al.* 1978). In this model it is assumed that a 'catastrophic' isotopic homogenization of the mantle has occurred which can be dated by the isochron.

These two types of model are not clearly related to each other and appear to be complementary.

In this paper, we wish to review the significant chemical and isotopic data relevant to mantle heterogeneity. We shall develop a model of continuous mantle evolution which relates geochemical observations to geodynamic models, and takes into account such factors as the chemical and isotopic changes that result from mantle convection processes, the progressively reducing rate of convection with time, and the extraction and growth of continental crust.

Part I. Review and comments on relevant observations

1. *Isotope and trace element geochemistry of the present mantle*

Present observations are based on data from basalt and peridotite samples. Both types of sample result from specific complex processes sampling different parts of the mantle, but it is important to note that the sampling occurs on very different scales.

(*a*) *Radiogenic isotope variations in basalts*

The analysis of radiogenic isotope variations is now mainly based on two coupled systems: the neodymium–strontium correlation and lead isotope systematics. Both systems appear to be internally consistent, but the relation between them remains obscure.

The neodymium–strontium correlation. Richard *et al.* (1976) first measured variations of the neodymium isotopic composition in basalts and showed that Sr and Nd variations were inversely correlated. Since then, this inverse correlation (figure 1*a*) has been well documented (DePaolo & Wasserburg 1976; O'Nions *et al.* 1977). Several domains can be distinguished on this correlation line: from higher to lower $^{143}Nd/^{144}Nd$ isotopic ratios domains for m.o.r.b., oceanic island basalts and continental basalts. However, each domain overlaps the next one, and the distribution of Sr and Nd isotope compositions is *continuous* on the correlation line.

Since the present $^{143}Nd/^{144}Nd$ ratio for chondrites and achondrites is known, the correlation diagram allows the $^{87}Sr/^{86}Sr$ ratio corresponding to a 'planetary' evolution in a closed system to be determined, and hence the Rb/Sr ratio for the Earth's mantle (DePaolo & Wasserburg 1976; O'Nions *et al.* 1977). The Nd and Sr isotopic results can then be expressed as relative deviations, ϵ_{Nd} and ϵ_{Sr}, from the planetary reference. Nd–Sr relations have been quantitatively investigated by Allègre *et al.* (1979*a*), who concluded that the correlation could be created by successive partial melting events in the mantle.

PHILOSOPHICAL TRANSACTIONS OF THE ROYAL SOCIETY A MATHEMATICAL, PHYSICAL & ENGINEERING SCIENCES

The lead isotope diagrams. Both $^{206}Pb/^{204}Pb$ and $^{207}Pb/^{204}Pb$ ratios integrate the chemical fractionation history of the U/Pb ratio. Uranium–lead fractionations older than, say, 2 Ga are traced equally by both ratios. However, because of the more rapid decay of ^{235}U, younger episodes of fractionation are only registered by the $^{206}Pb/^{204}Pb$ ratio. Most good quality data for lead isotopic composition in basalts are given in figure 1*b* (Sun & Hanson 1975*a*). Altogether, they define a large domain in the $^{207}Pb/^{204}Pb$–$^{206}Pb/^{204}Pb$ diagram. When restricted to geographical areas, the data define smaller domains which can even be approximated by straight lines (Canary Islands, North Atlantic m.o.r.b. (Sun *et al.* 1975; Sun & Hanson 1975*a*; Dupré & Allègre 1980); Hawaiian Islands (Tatsumoto 1978)). Thus, the data do not define a unique worldwide 'mantle isochron' but can possibly be interpreted by a series of local mantle isochrons. In any case, they tend to define several mantle domains which have had a different chemical evolution.

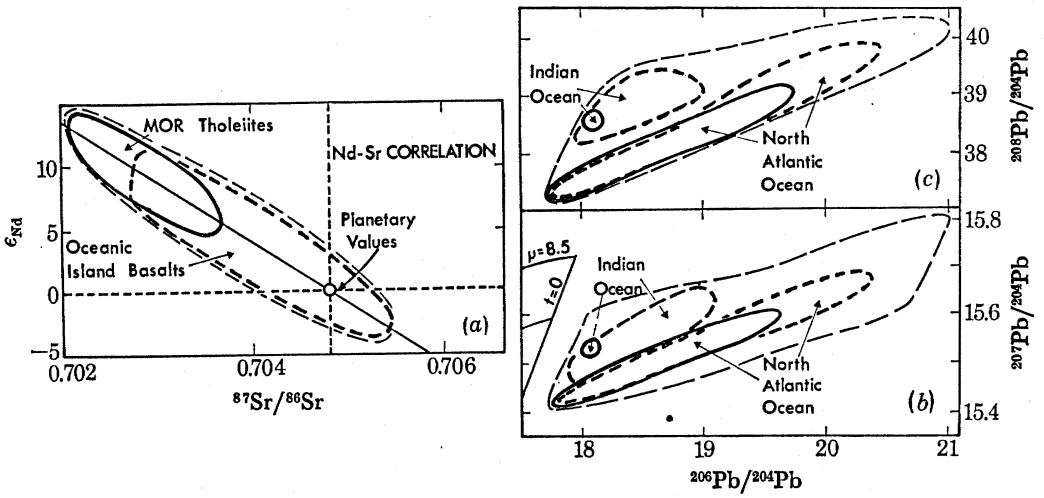

FIGURE 1. Isotopic correlations in modern oceanic basalts. The light dotted lines show the overall set of existing data. The heavy dotted lines correspond to the oceanic island basalts. M.o.r.b. are marked by the heavy lines. (*a*) Sr–Nd isotopic correlation. The Nd isotopic composition is expressed as deviation from the present chondritic value ($\epsilon_{Nd} = 0$). The areas for m.o.r.b. and oceanic island basalts clearly overlap. (*b*) $^{207}Pb/^{204}Pb$–$^{206}Pb/^{204}Pb$ diagram for oceanic basalts. The whole set of data defines a two-dimensional area. Good correlations can be described for individual oceans (here for the North Atlantic Ocean and the Indian Ocean). More precise correlations are found at a more local, regional scale (not shown on the figure). (*c*) Same as (*b*) for the $^{208}Pb/^{204}Pb$–$^{206}Pb/^{204}Pb$ diagram; (*b*) and (*c*) reveal uranium–lead fractionations older than 2 Ga.

As with the Nd/Sr correlation, an almost complete continuity is found between the various domains of figure 1*b*. However, the Pb isotope data show much more dispersion than do the Nd–Sr isotopes. In view of the chemical identity of the parent–daughter systems of the $^{206}Pb/^{204}Pb$ and $^{207}Pb/^{204}Pb$ ratios as opposed to that for $^{87}Sr/^{86}Sr$ and $^{143}Nd/^{144}Nd$, this might appear quite surprising.

Two processes can *a priori* be envisioned for this effect. Either

(1) the Pb isotope heterogeneity reflects an ancient isotopic heterogeneity of the mantle which could result from its primitive history, or

(2) the U/Pb chemical fractionation has varied with time. Owing to the difference between the ^{238}U and ^{235}U decay constants, this could have produced the present two-dimensional dispersion of Pb isotope ratios. In a $^{208}Pb/^{204}Pb$–$^{206}Pb/^{204}Pb$ diagram (figure 1*c*), the data do not define a single trend either. Since the decay constants of ^{232}Th and ^{238}U are similar compared to geological time scales, pure age effects cannot create a two-dimensional scatter in this diagram.

Thus, the combined data from figure 1*b* and *c* tend to indicate that Pb isotopic compositions were heterogeneous in the ancient mantle. This will be discussed later on.

Comparison between Pb–Pb *and* Nd–Sr *systematics*. In this section we compare briefly the Pb isotope data and the Nd–Sr systematics. Because data for Sr isotopic compositions are much more abundant than for Nd, we shall study the correlations between Sr and Pb isotopes (Sun & Hanson 1975*a*). The results are given in figure 2*a*. As for figure 1*b*, no clear worldwide correlation can be observed. On a regional scale, however, Sr and Pb isotopes are positively correlated in m.o.r.b. (figure 2*b*). This effect is discussed in a separate paper (Dupré & Allègre 1980). As for lead isotopes, these features can be related to purely time-related fractionations or to ancient heterogeneities. Following the same reasoning, a comparison between $^{207}Pb/^{204}Pb$–$^{87}Sr/^{86}Sr$ and $^{206}Pb/^{204}Pb$–$^{87}Sr/^{86}Sr$ diagrams indicates that, in addition to some possible time effects, an ancient lead isotope heterogeneity is probably involved.

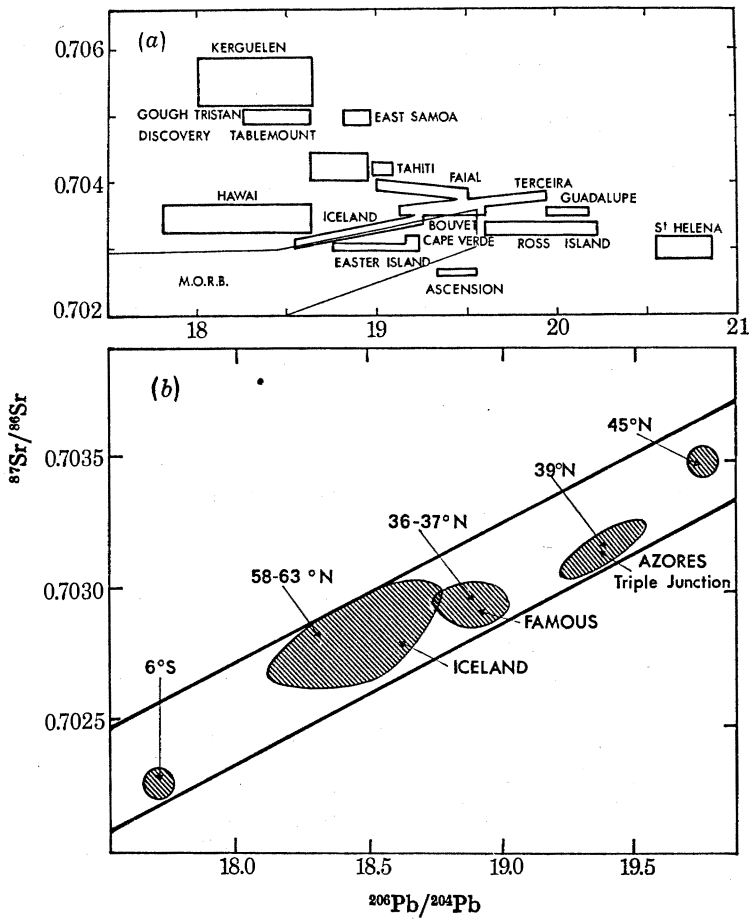

FIGURE 2. $^{87}Sr/^{86}Sr$–$^{206}Pb/^{204}Pb$ diagram for oceanic basalts. (*a*) Oceanic island basalts appear uncorrelated, although a more positive correlation can be found for a given island (modified from Sun & Hanson 1975*a*). (*b*) The data for North Atlantic m.o.r.b. yield a well defined positive correlation.

(*b*) *Trace element variations in basalts*

Following Treuil (1973) and Bougault *et al.* (this symposium), the only trace element ratios that can be considered as representative of the mantle source regions are ratios of hygromagmatophile elements (hyg. elements): Pb, U, Th, Rb, K, Ba, Ta, Nb, Hf, Zr, La, Ce, Nd and Sm.

The K–Rb *relation.* The old problem of the variations of the K/Rb ratio in basalts (see, for example, Gast 1968) has not yet been solved. K/Rb approximately equals 800–1500 in tholeiites, whereas it is about 200 in alkali basalts. According to the above discussion, if partial melting is in equilibrium, two different mantle sources should be considered for these basalts.

Rare earth elements. As emphasized by Gast (1968), the r.e.e. patterns of alkali basalts are light-r.e.e. enriched whereas those in m.o.r.b. are light-r.e.e. depleted. Since the light r.e.e. can be considered as hyg. elements, this feature is a characteristic of the mantle sources of these basalts; whereas the latter result is in agreement with the neodymium isotopic composition of m.o.r.b. the former is less clearly related to the positive ϵ_{Nd} characteristics of alkali basalts.

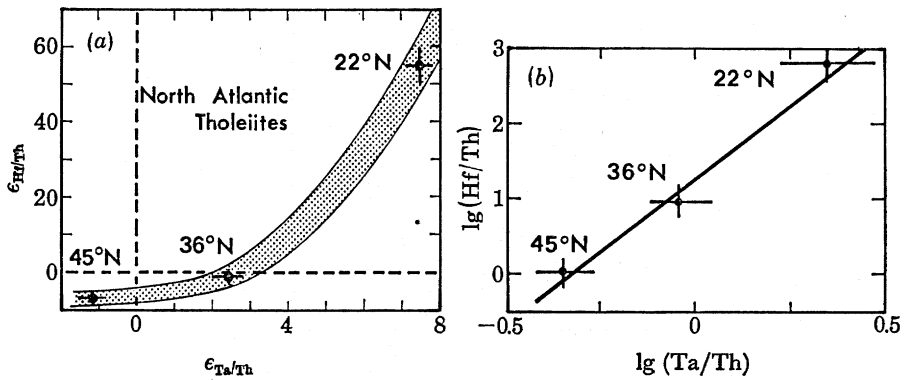

FIGURE 3. Hf/Th–Ta/Th diagram for North Atlantic m.o.r.b. The data are expressed as deviation from the chondritic values: $Ta/Th_{ch} = 0.8$; $Hf/Th_{ch} = 3$ (Joron, personal communication). Such ratios are not expected to be significantly fractionated during equilibrium partial melting and fractional crystallization. These variations are thus representative of mantle heterogeneity. In this diagram, mixing yields a straight line. As a consequence deviation from a given ratio implies the formation of a residual domain presenting the opposite variation. In (*b*) the same data are shown, plotted logarithmically.

Ta, Th, Hf, Nb, Zr *and* Y. Treuil & Joron (1975), Bougault *et al.* (this symposium) and Wood *et al.* (1979) have studied the variations of these trace element ratios in basalts. Whereas Nb/Ta, Zr/Hf ratios appear constant and chondritic in North Atlantic basalts, some other ratios (e.g. Ta/Th and Ta/Hf) vary along the Mid-Atlantic Ridge (M.A.R.). This observation is considered further in Part II.

Variations of trace element ratios can be expressed as deviations from the chondritic ratios (e.g. $\epsilon_{Ta/Th} = 10(Ta/Th_{sample} - Ta/Th_{chondrites})/Ta/Th_{chondrites}$). The multiplier factor emphasizes the scale of the variations. An example of the correlation between Ta/Th and Hf/Th variations is given in figure 3. In such a diagram, mixing results in a straight line. As a consequence, starting from a mean chondritic Earth, deviation from this ratio in a given domain results in residual domains with opposite variations.

(*c*) *Trace element–radiogenic isotope relations*

Mantle isochrons. Tatsumoto (1966) and Sun & Hanson (1975*a*) noted that variations of the daughter isotopic ratios ($^{206}Pb/^{204}Pb$ or $^{87}Sr/^{86}Sr$) were correlated with those of the parent/daughter element ratios ($^{238}U/^{204}Pb$ and $^{87}Rb/^{86}Sr$, respectively). These features have been interpreted as isochrons dating a major chemical fractionation in the mantle (Sun & Hanson 1975*a*; Brooks *et al.* 1976). It is known, however, that Rb and Sr as well as U and Pb fractionate during basalt genesis, for small degrees of partial melting. Secondly, the Rb/Sr and U/Pb ratios

can be modified by continental crust contamination or seawater alteration. Thus, mantle isochrons are at best significant for fresh tholeiites only (Brooks *et al.* 1976). The ^{87}Rb–^{87}Sr age determined by such a 'mantle isochron' is around 1.6 Ga, similar to that determined from lead isotopes (Sun & Hanson 1975*a*).

However, a rather poor correlation is found between $^{143}Nd/^{144}Nd$ and $^{147}Sm/^{144}Nd$ ratios in basalts. This can be attributed to the behaviour of Sm and Nd during petrogenetic processes. Moreover, for the M.A.R., ^{147}Sm–^{143}Nd model ages are 1.1 Ga, i.e. much younger than the age of ^{87}Rb–^{87}Sr mantle isochrons (Carlson *et al.* 1978). All considered, we believe that mantle isochrons are at best one interpretation of these isotope–trace element correlations in basalts, but we shall discuss this point later.

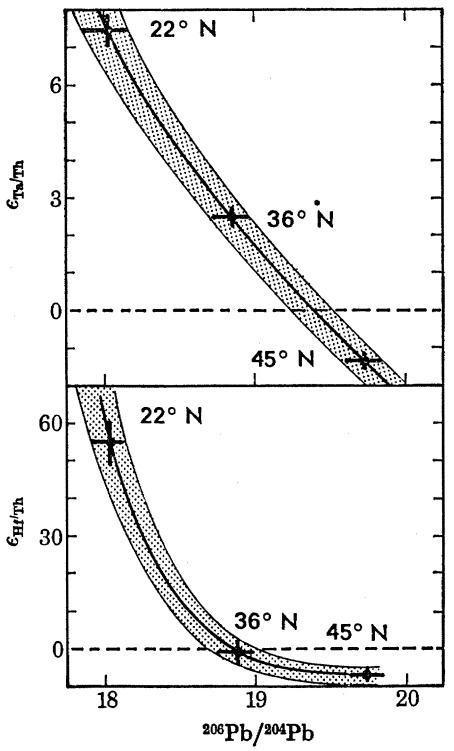

FIGURE 4. Isotope–trace element correlation. For example, negative correlations are observed in North Atlantic m.o.r.b. between the $^{206}Pb/^{204}Pb$ isotopic ratio and the hyg. element ratios such as Ta/Th and Hf/Th. This indicates that several episodes, rather than one major episode, have created the isotopic heterogeneities.

Radiogenic isotope–hyg. element correlations. An interesting correlation can be observed between lead, strontium and neodymium isotopic compositions and hyg. element ratios along the M.A.R. (Dupré & Allègre 1980). An example of this correlation is given in figure 4. Since several partial melting events are needed to fractionate these hyg. element ratios significantly, this correlation may indicate that the isotope variations result from progressive effects, rather than from major catastrophic episodes of chemical fractionation in the mantle.

(*d*) *Geochemical relations in ultramafic rocks*

Two main types of ultramafic samples will be considered here: orogenic lherzolites and ultramafic nodules in kimberlites and basalts.

Orogenic lherzolites. Trace elements and radiogenic isotopes have been extensively studied in

orogenic lherzolites (Frey 1969; Loubet *et al.* 1975; Menzies & Murthy 1978; Dupré *et al.* 1979; Polvé & Allègre 1980; Richard & Allègre 1980). R.e.e. systematics in Lanzo, Beni Bousera and Lherz (Loubet *et al.* 1975) reveal three main aspects of the formation of these massifs. Orogenic lherzolites are residues of 5% partial melting of a light-r.e.e. depleted peridotitic material. They have suffered a complex history, including several episodes of partial melting and local fractional crystallizations. Large variations in r.e.e. concentrations occur within a single massif on a scale of tens of metres. These results are supported by recent analyses of radiogenic isotopes. Sr, Nd and Pb isotopic compositions are close to m.o.r.b. type values (Polvé & Allègre 1980; Menzies & Murthy 1978; Richard & Allègre 1980; Dupré *et al.* 1979). $^{87}Sr/^{86}Sr$ and Rb/Sr analyses of diopsides and whole rocks in lherzolitic massifs (Menzies & Murthy 1978; Polvé & Allègre 1980) reveal local heterogeneities on the scale of rock samples and multi-episode chemical fractionations. In addition, by the use of mean Rb/Sr ratios, variations of the $^{87}Sr/^{86}Sr$ isotopic ratio indicate a time scale of chemical fractionation of the order of 10^9 years.

With the important and critical exception of K, Rb, Ba and probably Cs, isotope and r.e.e. patterns of these samples have m.o.r.b. source type characteristics (Menzies & Murthy 1978).

Xenoliths in basalts and kimberlites. One important feature of xenoliths in basalts and kimberlites is that they have been contaminated by their host magmas and possibly by fluid phases in reaction with the magma. This was first demonstrated by Shimizu (1975) on the basis of $^{87}Sr/^{86}Sr$ analyses of xenoliths in Hawaiian basalts and in kimberlites from Lesotho. This contamination has apparently affected r.e.e. also (Shimizu 1975) and explains why r.e.e. patterns are generally light-r.e.e. enriched in such xenoliths (see, for example, Frey & Green 1974).

Thus these xenoliths should be studied through their mineral separates, rather than by whole rock analysis. Two important results have been obtained by such studies. First, some trace elements (light r.e.e., Ti, etc.) are enriched in some nodules relative to some others (Frey & Prinz 1978; Shimizu & Allègre 1978). This enrichment is not correlated in a simple way with the structural types (granular and sheared). This result might indicate that trace element fractionation in nodules is controlled by several processes; depletion might result from partial melting. Enrichment could be created by metasomatism as proposed by Gurney *et al.* (1977) and Erlank & Rickard (1977). Secondly, strontium isotopic compositions are in equilibrium in granular nodules. Conversely, the isotopic compositions of Pb, Sr and Nd are heterogeneously distributed in minerals from sheared and volcanic nodules (Kramers 1979; Allègre *et al.* 1978). They are of m.o.r.b. type in diopside, whereas they are more radiogenic in garnet. In addition, when studying these minerals in a $^{87}Rb/^{86}Sr$–$^{87}Sr/^{86}Sr$ diagram, garnet and diopside define two point lines, the slope and intercept of which are negatively correlated. This can be understood if the $^{87}Rb/^{86}Sr$ system is controlled by exchanges between these two minerals and progressive re-equilibrium (Allègre *et al.* 1978).

Conclusions. The trace element and radiogenic isotope characteristics of basalts can be created by partial melting of ultramafic materials. The main difficulty concerns the alkali elements, which are generally not concentrated enough in the latter to satisfy the concentrations observed in the former. As discussed by Beswick (1976) and Menzies & Murthy (1978), K, Rb and Ba concentrations and K/Rb ratios in basalts can be explained if some phlogopite or amphibole is stable in the upper mantle.

The heterogeneity of the mantle which can be deduced from basalts is indeed observed in ultramafic materials. The latter is, however, a small-scale heterogeneity between the various minerals. Ultramafic materials (nodules and orogenic lherzolites), which can be samples of the

PHILOSOPHICAL TRANSACTIONS OF THE ROYAL SOCIETY A MATHEMATICAL, PHYSICAL & ENGINEERING SCIENCES

ultramafic lithosphere, have been altered by several episodes of magmatic processes during a time scale of gigayears. This observation is consistent with the idea of recycling of lithospheric material, as deduced from sea-floor spreading models.

2. *The ancient Earth mantle*

Data concerning isotope and trace element concentrations in the ancient mantle are scarce. Fresh basalts are extremely rare in the older geological record and equivalence between petrological associations is doubtful (e.g. greenstone belts = islands arcs?). Reliable results are obtained only for elements resistant to alteration (Zr, Hf, Th, Ta, Nb, and the r.e.e.), and by analysing unalterable minerals like diopside (Hart & Brooks 1977).

(*a*) *Radiogenic isotopes*

The initial Nd isotopic compositions of almost all Precambrian greenstone belt lavas and Precambrian crustal rocks follow a planetary evolution line (DePaolo & Wasserburg 1976; O'Nions *et al.* 1978; Zindler *et al.* 1978). This supports the concept of closed system behaviour. Results for Sr are less clear, but seem also to follow the same rule, that is they are less dispersed around the planetary line than modern values. As shown by Manhes *et al.* (1980), lead isotopes do not follow such a rule and are as dispersed in Precambrian rocks as in modern ones.

(*b*) *Trace elements*

Estimation of trace element concentrations in the Precambrian mantle are provided by Archaean komatiitic lavas (see, for example, Hart *et al.* 1970; O'Nions & Pankhurst 1978; Sun & Nesbitt 1977). These lavas are formed by large degrees of partial melting and therefore their hyg. element ratios are reliable estimates of their mantle source. Whereas few reliable data are available to provide absolute abundances, one can estimate a few hyg. element ratios, for example Zr/Ti = 100, Hf/Th = 8–11, Ta/Th = 0.8–1.2, Rb/Sr = 0.035, La/Sm = 0.7–1.3 (Hart *et al.* 1970; Sun & Nesbitt 1977; Bougault *et al*, this symposium; J. L. Joron, personal communication). Those trace element ratios that have varied since the Precambrian are also those that show present geographic variations (Bougault *et al.*, this symposium).

Part II. Qualitative and quantitative speculations

1. *The generation of chemical heterogeneities in the mantle*

The chemical heterogeneity of the mantle may *a priori* be explained by two models.

(*a*) It represents an initial heterogeneity, created perhaps during heterogeneous accretion, which might have survived the continuous stirring effects of mantle convection.

(*b*) That the heterogeneity has been created through geological time from an initially homogeneous mantle. In such a model, the present state is a balance between the processes that create heterogeneity and convection which erases it.

Evidence can be found for both models. $^{129}Xe/^{130}Xe$ variations in mantle materials are necessarily a remnant of an early heterogeneity (Boulos & Manuel 1971; Rison & Kyser 1977). Similarly, the apparent variations in lead isotope ratios in the Precambrian mantle, though not yet understood, might result from an initial heterogeneity in the mantle. On the other hand the essentially chondritic evolution curves of both Nd and Sr isotopes before 1 Ga tend to argue in favour of a well-mixed Precambrian mantle.

PHILOSOPHICAL TRANSACTIONS OF THE ROYAL SOCIETY A MATHEMATICAL, PHYSICAL & ENGINEERING SCIENCES

We shall demonstrate that the second model can explain most of the features observed for radiogenic isotope and trace element data in the present mantle. In this section, we shall first qualitatively examine the processes that may have created chemical heterogeneities as well as those that may have homogenized the mantle. These processes are obviously connected with mantle convection and its evolution with time.

(*a*) *Generation of heterogeneities*

Heterogeneities created during sea floor spreading. During the upwelling process which creates the oceanic lithosphere, some magmatic liquid segregates and leaves behind a residual solid. The liquid is enriched in incompatible elements, and forms the oceanic crust. The residual refractory solid is correspondingly depleted in incompatible elements. Hereafter the term 'positive anomaly' will be used for a heterogeneity corresponding to an enrichment of incompatible elements, and 'negative anomaly' for the corresponding depletion. Thus the oceanic lithosphere carries layers of both positive and negative anomalies. For some trace elements, the differences between these anomalies can be of several orders of magnitude.

Chemical effects during sea floor alteration. The upper part of the oceanic crust exchanges with seawater. Thus compositions of trace elements (Cl, Na, K, Rb, Cs, Sr) as well as the isotopic composition of Sr are modified in the oceanic crust during its transit between ridge and subduction zone. By contrast, no significant isotopic differentiation can be created between the different layers of the lithosphere during the mean 100 Ma life span of the plate. For example, by using extreme Rb/Sr ratios in m.o.r.b. and high temperature peridotites, a maximum differential growth in $^{87}Sr/^{86}Sr$ of only 0.000 05 is created in 100 Ma.

Heterogeneities created at subduction zones. At subduction zones, both the altered oceanic crust and the positive and negative anomaly-bearing layers are reinjected into the mantle. In addition, some sediments might be dragged into the mantle by the subducting oceanic lithosphere (Armstrong 1968). Although oceanographic evidence has generally been in disagreement with this model (e.g. that of Le Pichon *et al.* 1973), the results of recent deep-sea drilling in the Western Pacific seem to support such a process. For example, no compressional effect is found in trench sediments. Secondly, sediments interbedded with basalt flows are observed. Such subducted sediments may have a dual origin: some are volcanogenic but other detrital or pelagic sediments may have a continental origin. Both are enriched in incompatible elements and radiogenic isotopes and might create a positive anomaly in the mantle. On the other hand, island arc or continental margin volcanism creates a negative anomaly in the residual mantle source regions.

Preservation of heterogeneities after subduction. The subducted plate that penetrates into the mantle is a sandwich of positive and negative chemical anomalies. The magnitude of the chemical anomalies will decrease with time as a result of convective and diffusion processes, but nevertheless isotopic heterogeneities will be generated through radioactive decay as long as these heterogeneities persist. The order of magnitude of the isotopic effects thus depends on the lifetime of this material in the mantle. Given a total ridge length of about 6×10^4 km, a mean spreading velocity of 3 cm/a, and a mean thickness of the oceanic lithosphere of 70 km, then the volume of lithosphere which is reinjected into the mantle is 1.3×10^{17} cm^3/a. The whole mantle volume is 9.0×10^{26} cm^3.

Thus, if convection affects the whole mantle, the residence time of lithospheric plate in the mantle is 7 Ga. If convection affects a 1000 km layer of the upper mantle, the residence time of

PHILOSOPHICAL TRANSACTIONS OF THE ROYAL SOCIETY A MATHEMATICAL, PHYSICAL & ENGINEERING SCIENCES

this material in the mantle is about 3 Ga. Assuming that convection was more active in the past, the residence time might have been shorter, of the order of 1–2 Ga. Nevertheless, the abundance of radiogenic isotopes will increase significantly. For instance if, at the beginning of a 'cycle', two adjacent reservoirs have similar isotopic ratios but different parent: daughter ratios, their isotopic ratio will be significantly different at the end of the cycle.

Global budget constraints and continental crust formation. In general, the same number of positive and negative anomalies are created in the mantle by the previous processes. However, the opposite is observed in the Earth: the mantle is depleted in incompatible elements and shows a mean negative anomaly compared with the continental crust which is enriched in these elements. Thus, a part of the positive anomalies created along ridges or trenches should be stored in the continental crust, creating an opposite negative anomaly in the mantle.

Whereas this process can create the mean chemical depletion observed in the mantle, it is possible that local positive anomalies resulting from the subduction of sediments or of oceanic crust can survive locally in the mantle. Second-order positive anomalies can thus be created in such a way.

Mineralogical heterogeneities. Trace element ratios vary in the different minerals. For example, the Rb/Sr ratio is higher in garnet than in diopside. Therefore, in a given mineral assemblage initially formed in isotopic equilibrium, some isotopic disequilibrium will be created by radioactive decay. If diffusion is slow enough, large isotopic differences can be created with time. Indeed $^{87}Sr/^{86}Sr$ isotopic ratios varying from 0.7022 in diopside to 0.710 in garnet have been recorded in ultramafic nodules (Allègre *et al.* 1978). Thus, mineral assemblages may exist that are equilibrated for major and trace elements, but disequilibrated for radiogenic isotopes. This isotopic disequilibrium may be erased at high degrees of mantle melting, but it is possibly significant at low degrees of melting and may convey isotopic variations to the melt.

(*b*) *Destruction of heterogeneity*

In a convecting mantle, the chemical heterogeneity can be erased by either diffusion or advection. The general equation that describes the evolution with time t of the concentration C_i of element i can be written

$$\partial C_i/\partial t = D_i \nabla^2 C_i - v(x, y, z, t)\, \nabla C_i + Q_i(x, y, z, t), \qquad (1)$$

where D_i is the diffusion coefficient of element i, and v is the velocity vector for convection which depends on the spatial coordinates x, y, z, and on time t. The first term of the right-hand side of (1) describes the process of diffusion of element i in the mantle material. The second term corresponds to advection. Q_i is the source term, which describes the creation of heterogeneity by the processes previously mentioned and by radioactive decay.

Diffusion. As discussed by Hofmann & Hart (1975), the diffusion coefficients of trace elements in solid mantle type materials are within a few orders of magnitude of 10^{-13} cm^2/s. It is possible that D is larger at greater mantle depths, of the order of 10^{-10} cm^2/s. During a time t, the characteristic distance of diffusion of a trace element in the solid mantle is thus $x = (Dt)^{\frac{1}{2}}$; during 1 Ga, it is 50–1700 cm. Thus solid diffusion in the mantle can create only local equilibrium on the scale of $\frac{1}{2}$ m in the upper mantle, or 20 m in the lower mantle. In particular, this process *cannot* result in 'dissolution' of subducted plates into the bulk mantle.

Conversely, diffusion coefficients of trace elements in silicate liquids are of the order of 10^{-7} cm^2/s, which might achieve diffusion distances of about 600 m within 1 Ga. A small (1 mm)

PHILOSOPHICAL TRANSACTIONS OF THE ROYAL SOCIETY A MATHEMATICAL, PHYSICAL & ENGINEERING SCIENCES

grain will equilibrate with a silicate liquid within 10 ka (Hofmann & Hart 1975). However, if the medium is enriched with some gas fluid phase (in particular in a supercritical state), the diffusion coefficient is of the order of 10^{-4} cm^2/s and the time scale of equilibration would be considerably shortened. Thus if partial melting is involved at any stage during a convective cycle, such as in the low-velocity zone, it can be assumed that the mineral assemblages are chemically and isotopically equilibrated.

Advection. Potentially, advection is far more efficient than diffusion. Characteristic distances of exchange are approximately $x = Vt$. If an approximate rate of mantle convection of 1 cm/a is assumed, a characteristic distance of exchange of 10^4 km is attained within 1 Ga. This would induce a large-scale rehomogenization of the mantle.

In fact, the advection process is efficient only in the direction of the stream. In a lateral direction, homogenization depends on secondary transfers. Numerical modelling of mantle convection (Richter 1973; MacKenzie *et al.* 1974; Richter & MacKenzie 1978) indicates that homogenization occurs on several scales. In this case, chemical homogenization can be described by an eddy diffusion process and an eddy diffusion coefficient D_e. If one assumes that 100 km domains are homogenized within 100 Ma, as Richter & Ribe (1979) seem to claim, then D_e would be about 3×10^{-2} cm^2/s. Values such as 10^{-3} or 10^{-4} cm^2/s do not appear unreasonable.

Homogenization is, however, not necessarily attained at all on regional scales: all tectonic structures of mantle materials are elongated and laminar. This is true of the fine-scale structures of peridotitic xenoliths in basalts and kimberlites and of high temperature peridotites. This indicates that convection is only effective at relatively large scales, say larger than 1000 m. Thus chemical and isotopic homogenization at smaller scales is always controlled by diffusion, and cannot be attained during geological time scales.

In conclusion, it is emphasized that advection can be a very efficient process for mantle homogenization at intermediate and large scales (say larger than 1000 m). For smaller scales (centimetres to a few tens of metres), chemical and isotopic exchanges are controlled by diffusion, which is a very slow and inefficient process under mantle conditions.

(*c*) *Scales of heterogeneities*

Following the above discussion, it is necessary to define the scales of the chemical and isotopic heterogeneity of the mantle in space and time.

Heterogeneity in space. The problem here is to decipher the scale of mantle heterogeneity. Is the mantle uniform for ocean-scale domains (e.g. Atlantic, Pacific, Indian Ocean) but heterogeneous on a scale of metres? Or rather is the mantle homogeneous at the kilometre scale, but chemically varying from one domain to the other? The different possible cases are schematized in figure 5.

According to the first type of model, the present mantle is heterogeneous on a small (mineral) scale but homogeneous at all larger scales. Indeed, both mantle nodules and high-temperature peridotites show evidence of isotopic disequilibrium between minerals as well as between different whole rock samples from a given nodule or ultramafic body (Stueber & Ikramuddin 1974; Basu & Murthy 1977; Kramers 1979; Allègre *et al.* 1978). The time scales of these heterogeneities can be estimated from the isotopic heterogeneities: they range from 3 Ga in nodules from California (Basu & Murthy 1977) to 1.7 or 0.9 Ga in nodules from Lesotho kimberlites (Allègre *et al.* 1979*b*) and high-temperature peridotites from Lherz (Polvé & Allègre 1980). As discussed previously, Sr and Pb isotopic compositions are more radiogenic in garnet than in diopside from such materials: $^{87}Sr/^{86}Sr$ ratios range from 0.702 to 0.703 in diopside and from

PHILOSOPHICAL TRANSACTIONS OF THE ROYAL SOCIETY A MATHEMATICAL, PHYSICAL & ENGINEERING SCIENCES

0.705 to 0.710 in garnet whereas $^{206}Pb/^{204}Pb$ ratios range from 18.05 to 18.5 in diopside, and from 19.0 to 21.0 in garnet. Therefore, for small degrees of disequilibrium partial melting, in which relatively large amounts of garnet enter the melt, isotopic compositions typical of alkali basalts can be obtained. For larger degrees of melting involving large quantities of diopside, less radiogenic values typical of ocean basalts will be obtained. If phlogopite is involved, such a model can also explain the differences in K/Rb ratios between m.o.r.b. and alkali basalts (see discussion by Griffin & Murthy 1969).

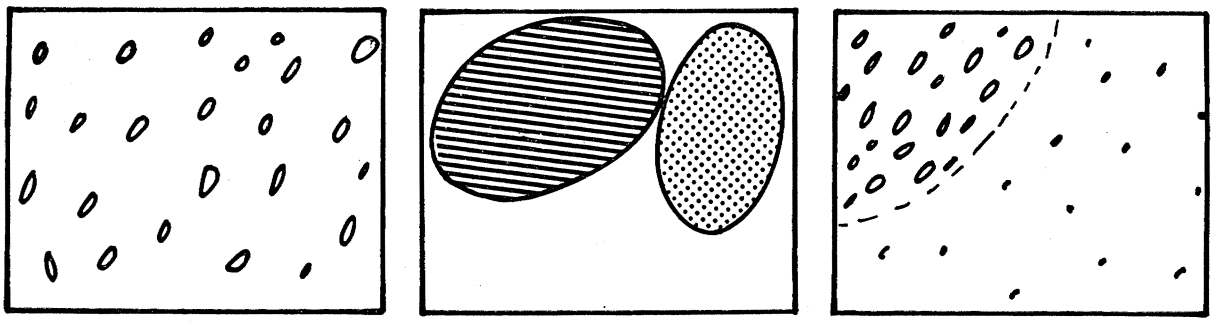

model I: large-scale homogeneities; small-scale heterogeneities

model II: large-scale heterogeneities; small-scale homogeneities

model III: large-scale heterogeneities; small-scale heterogeneities

FIGURE 5. Schematic diagram showing the possible scales of mantle heterogeneity. The first type of model describes a mantle homogeneous on a large scale but heterogeneous on the mineral scale. Variations in basalts mainly result from disequilibrium partial melting. For the second type of model, the mantle is homogeneous on a small scale, but is divided into large domains of variable composition. Variations in basalts result from sampling of these different domains. Present data tend to support a third type of model where the mantle is heterogeneous on both small and large scales.

Nd isotopic compositions of alkali basalts and m.o.r.b. are not explained by disequilibrium partial melting of only garnet and diopside. Beswick & Carmichael (1978) proposed that the Nd isotope variations could be obtained by disequilibrium melting of the phosphate minerals apatite and whitlockite. In addition, this could also explain some of the differences in the r.e.e. patterns of alkali basalts and m.o.r.b.

Hofmann & Hart (1978) discussed the melting process of such disequilibrated materials. They concluded that, in view of the high diffusion coefficient values in magmatic melts, alkali basalts and tholeiites could not be created by this process. They inferred that the finding of two geochemically contrasted types of basalts (m.o.r.b. and alkali basalt) in close association required a vertical stratification of the Earth's mantle. This conclusion is not, however, self-evident. In large old oceans like the Pacific and South Indian Oceans, the oceanic island basalts are isotopically very similar to m.o.r.b. This is particularly true of Hawaiian basalts (O'Nions *et al.* 1977; Tatsumoto 1978). At the opposite extreme, large differences are found between oceanic island basalts and m.o.r.b. in the younger (200 Ma) Atlantic Ocean.

At the other extreme, there are the two-reservoir mantle models. Alkali basalts are envisaged to come from deep homogeneous sources, whereas tholeiites result from the melting of an upper convective reservoir. The chemical arguments can be summarized as follows. Incompatible elements are enriched and Nd and Sr isotope ratios are closer to bulk Earth or 'planetary' values in alkali basalts. Conversely, normal m.o.r.b. are depleted in incompatible elements and thus Sr and Nd isotopic compositions are fractionated relative to bulk Earth or planetary values.

PHILOSOPHICAL TRANSACTIONS OF THE ROYAL SOCIETY A MATHEMATICAL, PHYSICAL & ENGINEERING SCIENCES

However, lead isotopes have an 'open system' signature in many ocean island basalts, whereas they seem to have followed a planetary evolution more closely in m.o.r.b. sources. This can be reconciled by the following assumption. Let us suppose that the mantle was convecting as a whole during the Precambrian. During this period, Rb and Sr and Sm and Nd were not fractionated but U and Pb were fractionated by some process such as sulphide segregation into the core. Then the upper mantle was separated some 2 Ga ago. During this process Rb and Sr and Sm and Nd were fractionated, whereas U and Pb were not. Further, the stirring upper mantle from which continental crust had been extracted constituted the source for m.o.r.b. In addition, it may have been divided into large convection cells between which chemical exchanges are minimal. Conversely, the isolated lower mantle was not convecting and ancient lead isotope heterogeneities persisted. This part of the mantle is currently sampled by oceanic island basalts.

Green (1971) and Allègre & Bottinga (1974) have proposed a different model for large-scale mantle heterogeneities. They considered that alkali basalt sources are the result of liquid segregation and mantle metasomatism (Gurney *et al.* 1977). In the upper part of the asthenosphere, layers of magmatic liquid may form, which are variably enriched in incompatible elements. Such fertile zones or pockets may be tapped when cracks are formed in the lithosphere. Such a model is supported by the occurrence of light-r.e.e. enriched mantle xenoliths in kimberlite pipes (see, for example, Shimizu & Allègre 1978).

All things considered, it appears that the mechanisms of formation of alkali basalts are still imperfectly understood. Conversely, mid-ocean ridge basalts, which are by far the most abundant, can be reasonably considered as samples of a regionally homogeneous mantle. Their formation is clearly related to convection and sea floor spreading. In addition, such basalts are found in any geological period.

We shall try hereafter to model quantitatively the chemical and isotopic heterogeneities of the convecting mantle mainly on the basis of m.o.r.b. data. In addition, we shall constrain our model by reference to Archaean basaltic lavas, which we consider to be comparable with m.o.r.b. and good representatives of the geochemical character of ancient mantle.

Heterogeneity in time. The time scales of chemical heterogeneities can be deduced from the observed variations in isotopic compositions. Two different concepts should be considered. The first is the time necessary to create the spread of values around a mean value for normal m.o.r.b. The second is the time required to evolve the present typical isotopic ratios starting from a 'planetary' (chondritic) chemical system.

The second type of evolution relates to the mean present deviation in the Nd and Sr isotopic compositions of m.o.r.b. from calculated bulk Earth values. The time scale necessary for creating this deviation is at least 1–1.5 Ga. Note that this time scale is of the same order of magnitude as that for the creation of isotopic disequilibrium between minerals in ultramafic nodules.

The present spread of $^{87}Sr/^{86}Sr$ ratio in m.o.r.b. ($\Delta^{87}Sr/^{86}Sr = 0.0012$) can be created within 300 Ma if a maximum estimated variation of the mantle $^{87}Rb/^{86}Sr$ ratio of 0.3 is assumed. Chemical heterogeneity in Archaean mantle sources can be deduced from the r.e.e. compositions of tholeiitic and komatiitic lavas in Archaean greenstone belts. However, these ancient variations in r.e.e. patterns did not result in variations of the Nd isotopic composition (Zindler *et al.* 1978; Hamilton *et al.* 1977). The maximum possible departure of this Nd isotopic composition from a planetary value indicates that the time scale of these chemical heterogeneities was less than 30 Ma. Although these estimates are approximate, they provide us with important orders of magnitude for the critical parameters of our model.

PHILOSOPHICAL TRANSACTIONS OF THE ROYAL SOCIETY A MATHEMATICAL, PHYSICAL & ENGINEERING SCIENCES

2. *Quantitative chemical model of a convective mantle*

(*a*) *General formalism*

In this section we develop a model which describes the evolution of trace elements and radiogenic isotopes in a convecting mantle. As discussed above, we will only incorporate the features observed in m.o.r.b. We first establish a formalism for the mean mantle, and then consider that for mantle domains.

Mean mantle. As we have claimed, the chemical evolution of the mantle is mainly controlled by the magmatic fractionation of elements along mid-oceanic ridges. However, the process is rendered more complex by subduction, which recycles some oceanic crust into the mantle, but enables part of it to be extracted for continental growth. Afterwards, the oceanic crust is more or less mixed back into the underlying mantle.

Let us consider the amount x of an element in the mantle of volume V. It is possible to describe its variation $\mathrm{d}x$ as

$$\mathrm{d}x = -\mathrm{d}x_1(\text{ridge}) + \mathrm{d}x_2\,(\text{subduction}),$$

$$\mathrm{d}V = -\mathrm{d}V_1(\text{ridge}) + \mathrm{d}V_2\,(\text{subduction})$$

and

$$\mathrm{d}x_2 = ((1-fq)\,p)\,\mathrm{d}x_1,$$

$$\mathrm{d}V_2 = ((1-q)\,p)\,\mathrm{d}V_1,$$

where q is the fraction of oceanic crust that enters the continental crust, fq is the fractionation of the trace element during continental crust build-up and p is the fraction of oceanic crust that is mixed back into the mantle.

Along ridges, let us define the effective partition coefficient D between the solid mantle and the magmatic liquid extracted from it

$$\langle D\rangle = \frac{C_{\mathrm{m}}}{C_{\mathrm{liquid}}}\left(\frac{x}{V}\right)\Big/\left(\frac{\mathrm{d}x}{\mathrm{d}V}\right),$$

where C_{m} is the concentration of a trace element or a radiogenic isotope in the mantle and C_{liquid} is its concentration in the magmatic liquid. Then:

$$\frac{\mathrm{d}C_{\mathrm{m}}}{\mathrm{d}t} = \frac{\mathrm{d}}{\mathrm{d}t}\left(\frac{x}{V}\right) = C_{\mathrm{m}}\left(\frac{1}{G\langle D\rangle}-1\right)\frac{\mathrm{d}V}{V\mathrm{d}t}, \tag{2}$$

where

$$G = \frac{(1-q)\,p-1}{(1-qf)\,p-1}.$$

If the material reinjected into the mantle is rehomogenized, thus affecting the mean mantle, then $p = 1$. On the other hand, if the basaltic part of the reinjected material (with positive anomalies) is not rehomogenized into the mantle ($p = 0$), then the mean mantle evolution is only that of the residual mantle, in particular that of the lower part of the lithospheric plates that can be mixed efficiently because of its small mechanical contrast.

Integrating over the age of the Earth, and assuming that the mantle volume does not vary significantly,

$$\left|\int_0^t \frac{q}{V(\tau)}\frac{\mathrm{d}V}{\mathrm{d}t}(\tau)\,\mathrm{d}\tau\right| = \frac{V_{\mathrm{continent}}}{V_{\mathrm{mantle}}} = 6\times 10^{-3}.$$

If the process of continent formation began 4.0 Ga ago, then the mean value of $(q/V)\,(\mathrm{d}V/\mathrm{d}t)$ is $1.5\times 10^{-12}\,\mathrm{a}^{-1}$. However, the subducted oceanic crust, transformed to eclogite, probably does

PHILOSOPHICAL TRANSACTIONS OF THE ROYAL SOCIETY A MATHEMATICAL, PHYSICAL & ENGINEERING SCIENCES

not homogenize with the ultramafic mantle (Hofmann & Hart 1978) and may be considered as isolated from the system. The amount of oceanic crust that is subducted into the mantle is $\frac{5}{70}$ times that of oceanic lithosphere. According to the present spreading rate, this amounts to 10^{16} cm^3/a. Then $\mathrm{d}V/V\mathrm{d}t$ is 10^{-11} a^{-1}. If spreading rates were faster in the past (MacKenzie & Weiss 1975), it could be that $\mathrm{d}V/V\mathrm{d}t$ was of the order of 10^{-10} a^{-1}. Then q varies from 15 to 1.5%.

If the main process of liquid–solid fractionation is equilibrium partial melting, then

$$\langle D\rangle = \bar{D}+F(1-\bar{D}),$$

where F is the degree of melting, typically 10%, and $\bar{D}$ is the bulk partition coefficient of the residual solid. For example, for a hyg.-element (Treuil 1973), $\bar{D} = 0.01$ and $\langle D\rangle = 0.1$. Then, for a pure magmatic extraction model, $\varphi = (\langle D\rangle^{-1}-1)\,\mathrm{d}V/V\mathrm{d}t$ varies from 10^{-10} to 10^{-9} a^{-1}. For a more complex extraction model, we define $\bar{\varphi}^*$ as $\{(G\langle D\rangle)^{-1}-1\}\,\mathrm{d}V/V\,\mathrm{d}t$, which is of the order of magnitude of 10^{-10} a^{-1}.

Finally, note that if $\bar{\varphi}$ or $\bar{\varphi}^*$ is constant through time, (2) simply integrates into

$$C_\mathrm{m} = C_{\mathrm{m},0}\,\mathrm{e}^{\bar{\varphi}^* t},$$

where t is the time and $C_{\mathrm{m},0}$ the concentration of the element in the initial mantle.

Let us consider now the equation for chemical ratios, as deduced from (2). It is in particular desirable to describe the evolution of hyg.-element ratios. For two elements, i and j, (2) becomes

$$\frac{\mathrm{d}}{\mathrm{d}t}\left(\frac{C^i_\mathrm{m}}{C^j_\mathrm{m}}\right) = \frac{C^i_\mathrm{m}}{C^j_\mathrm{m}}\left(\frac{1}{G_i\langle D_i\rangle}-\frac{1}{G_j\langle D_j\rangle}\right)\frac{\mathrm{d}V}{V\,\mathrm{d}t}.$$

Let us define:
$$\bar{\psi}^{ij}(t) = \left(\frac{1}{G_i\langle D_i\rangle}-\frac{1}{G_j\langle D_j\rangle}\right)\frac{\mathrm{d}V}{V\,\mathrm{d}t} = \bar{\varphi}^*_i-\bar{\varphi}^*_j$$

and $r^{i,j}_\mathrm{m} = C^i_\mathrm{m}/C^j_\mathrm{m}$. Then
$$\mathrm{d}r^{i,j}_\mathrm{m}/\mathrm{d}t = \bar{\psi}^{i,j}(t)\,r^{i,j}_\mathrm{m}. \tag{3}$$

$\bar{\psi}^{i,j}$ generally varies with time. If, however, $\bar{\varphi}^{i}*$ and $\bar{\varphi}^{j}*$ are constant, (3) can easily be integrated.

When radioactive systems are considered, (3) for the parent/daughter chemical ratios r_m (e.g. ^{87}Rb/^{86}Sr, ^{238}U/^{204}Pb or ^{147}Sm/^{144}Nd) is transformed into

$$\mathrm{d}r_\mathrm{m}/\mathrm{d}t = \bar{\psi}(t)\,r_\mathrm{m}-\lambda r_\mathrm{m},$$

where λ is the decay constant of the parent nuclide.

The equation for the daughter isotopic composition α_m becomes

$$\mathrm{d}\alpha_\mathrm{m}/\mathrm{d}t = \lambda r_\mathrm{m},$$

where α_m can be, for example, ^{87}Sr/^{86}Sr, ^{206}Pb/^{204}Pb or ^{143}Nd/^{144}Nd.

In short, the evolution of a radioactive system in the mean mantle is described by the system of differential equations:

$$\left.\begin{aligned}\mathrm{d}\alpha_\mathrm{m}/\mathrm{d}t &= \lambda r_\mathrm{m}\\ \text{and}\qquad \mathrm{d}r_\mathrm{m}/\mathrm{d}t &= (\bar{\psi}-\lambda)\,r_\mathrm{m}.\end{aligned}\right\} \tag{4}$$

Such a system can easily be solved analytically for many types of $\bar{\psi}(t)$ functions.

Mantle domains. We can specify a mantle domain as a region of the mantle the points of which have all undergone the same chemical evolution. The mantle can *a priori* be divided into several domains that have not necessarily evolved in parallel with the mean mantle. These domains may bear chemical anomalies which can be created by continuous addition of sediments or

oceanic crust or by discrete events. These differences are erased by mixing with the surrounding mantle. The general equation, which describes the chemical evolution of such domains, is (1), but as discussed above, we can neglect the diffusion term of (1). In addition, we shall assume that mixing occurs between the domain and the mean mantle. We propose to transform (1) for a domain of variable volume into

$$\mathrm{d}C/\mathrm{d}t = (C_\mathrm{m} - C)\,R(t) - (\langle K\rangle^{-1} - 1)\,E(t)\,C + Q(t), \tag{5}$$

where $(C_\mathrm{m} - C)\,R(t)$ is the advection term of (1), C_m is the concentration of a trace element in the mean mantle, C is its concentration in a given domain, and $R(t)$ is the volumetric rate of mixing of the domain with the mean mantle. This can be considered equivalent to the ratio of the speed of displacement of the material to a typical size y of the domain. Then $(C_\mathrm{m} - C)/y$ corresponds to (∇C) in the advection term of (1). For mantle conditions, $R(t) \ll 1$. $Q(t) - (\langle K\rangle^{-1} - 1)\,E(t)\,C$ is the source term of (1), where $E(t)$ is the relative amount of material extracted from the domain per unit of time, and $\langle K\rangle$ is the effective partition coefficient of the element for this extraction. By analogy with (2), we define $\varphi(t) = -E(t)\,(\langle K\rangle^{-1} - 1)$, where $\varphi(t)$ can vary from one domain to another; $Q(t)$ is the relative amount of input of the trace element. It can be a continuous or an episodic function. This, in particular, includes radioactive decay.

Equation (5) can be transformed for the ratio $r^{i,j} = C^i/C^j$ of two elements i and j:

$$\mathrm{d}r^{i,j}/\mathrm{d}t = (r^{i,j}_\mathrm{m} - r^{i,j})\,L(t)\,R(t) + \psi^{i,j}(t)\,r^{i,j} + (r^{i,j}_\mathrm{ext} - r^{i,j})\,J(t), \tag{6}$$

where $r^{i,j}_\mathrm{m}$ is the ratio for the mean mantle, $L(t) = C^j_\mathrm{m}/C^j$, $(r^{i,j}_\mathrm{ext} - r^{i,j})\,J(t)$ describes the input into the domain from sources external to the mantle ($r^{i,j}_\mathrm{ext}$ is the ratio of element i to element j in these external sources, and $J(t)$ is the relative input of element j per unit time), and $\psi^{i,j}(t) = (\langle K^j\rangle^{-1} - \langle K^i\rangle^{-1})\,E(t) = \varphi^i(t) - \varphi^j(t)$.

For radioactive systems, (5) is transformed to the following systems of differential equations for the parent:daughter chemical ratio (r) and the daughter isotopic ratio (α):

$$\left.\begin{aligned} \mathrm{d}r/\mathrm{d}t &= (r_\mathrm{m} - r)\,L(t)\,R(t) + (r_\mathrm{ext} - r)\,J(t) + \psi(t)\,r - \lambda r;\\ \mathrm{d}\alpha/\mathrm{d}t &= (\alpha_\mathrm{m} - \alpha)\,L(t)\,R(t) + (\alpha_\mathrm{ext} - \alpha)\,J(t) + \lambda r. \end{aligned}\right\} \tag{7}$$

Before any further consideration, it appears that the two equations are coupled not only by radioactive decay but also by chemical fractionation. Therefore, some correlations may *a priori* exist between r and α, which would not only have an age significance.

In the next section we shall describe the chemical evolution of the residual mantle by (6) and (7). In these models the input term $J(t)$ will be neglected. This is equivalent to saying that the chemical evolution of the mantle source for m.o.r.b. has resulted only from magmatic extraction.

(*b*) *Steady-state behaviour*

As a first approximation, we consider that all coefficients are constant with time.

Mean mantle composition. We assume here that the values obtained by Hart *et al.* (1970), O'Nions & Pankhurst (1978), Sun & Nesbitt (1977), Joron & Treuil (1979) and Allègre *et al.* (1979*b*) for some magmatophile element ratios in Archaean greenstone belt lavas are representative of the 'mean' Archaean mantle, and that the present-day m.o.r.b. values are broadly representative of the present-day mantle values (table 1). Then we can compute the fractionation parameters $\overline{\psi}^{i,j}$ as

$$\overline{\psi}^{i,j} = (\Delta t)^{-1} \lg \frac{(C^i/C^j)_t}{(C^i/C^j)_{t+\Delta t}}.$$

Values for this parameter are given in table 1. Several remarks can first be made. It should be remembered that if the fractionation process is controlled by magmatic processes alone, then for a C^i/C^j ratio where C^j is more magmatophile than C^i, $\bar{\psi}^{i,j}$ is negative. Conversely, if C^j is less magmatophile than C^i, $\bar{\psi}^{i,j}$ is positive.

In agreement with the idea that solid–liquid partitioning is the dominant process, the values for $\bar{\psi}^{i,j}$ correspond to the following decreasing sequences of incompatibility: Cs > Ba > Rb > K > Sr (Hart 1971), La > Nd > Sm > Lu and Zr = Hf > Nb = Ta (Bougault *et al.*, this symposium).

TABLE 1. ARCHAEAN AND PRESENT HYG.-ELEMENT RATIOS CONSIDERED AS MEAN MANTLE VALUES

	2.7 Ga	present day	$\bar{\psi}_{2.7-\mathrm{now}}$/Ga
K/Ba	30	110	−0.481
K/Cs	5900	81000	−0.970
K/Rb	350	1046	−0.405
Rb/Sr	0.035	0.008	0.546
Ti/Y	250	290	−0.0549
Ti/Zr	100	100	0
Zr/Nb	22	5.1	0.540
Zr/Y	2.8	2.8	0
(La/Sm)†	0.9	0.55	0.22

For the source of data, see text. The evaluation of these ratios allows the estimation of the fractionation factors, $\bar{\psi}$, for the mean mantle, given in the last column. Positive values are obtained when the element in the numerator is more incompatible than that in the denominator. Those fractionation factors are used in figure 6.

† Normalized to chondrites.

It is also interesting to compare the variations of these ratios through time with the present geographical variations. For example, as shown by Bougault *et al.* (this symposium), the Zr/Hf ratio is constant in m.o.r.b., whereas Zr/Nb varies from one place to another. Similarly Zr/Hf is nearly constant through geological time, while Zr/Nb varies. Similar comparisons can be made for the other hyg.-element ratios.

Assuming for a given pair of elements that $G^i = G^j = G$, then

$$\bar{\psi}^{i,j} = (\langle D^i\rangle^{-1} - \langle D^j\rangle^{-1})\, G^{-1}\, \mathrm{d}V/V\,\mathrm{d}t.$$

In a plot of $\bar{\psi}^{i,j}$ against $(\langle D^i\rangle^{-1} - \langle D^j\rangle^{-1})$, where $\langle D^i\rangle$ and $\langle D^j\rangle$ are estimated from partition coefficient values, one should obtain a straight line of slope $G^{-1}\,\mathrm{d}V/V\,\mathrm{d}t$ (figure 6). For a pure magmatic model and 10% partial melting, no straight line can be obtained by using the current estimates of the bulk partition coefficients $\bar{D}$ of the trace elements. However, for an apparent degree of partial melting, F, of 1%, a straight correlation is obtained between the estimates of $\bar{\psi}^{ij}$ and $(\langle D^i\rangle^{-1} - \langle D^j\rangle^{-1})$ which yields a value for $G^{-1}\,V/\,V\,\mathrm{d}t$ of about $2 \times 10^{-11}\,\mathrm{a}^{-1}$. This is in agreement with the estimate of this parameter deduced from the present spreading rates when the oceanic crust is considered as isolated from the mantle. We shall return later with an interpretation for this value for F.

Other estimations of $\bar{\psi}$ can be obtained from isotopic ratios ($^{87}\mathrm{Sr}/^{86}\mathrm{Sr}$ or $^{143}\mathrm{Nd}/^{144}\mathrm{Nd}$). Equation (4) integrates to give

$$\alpha_{\mathrm{m}} = \alpha_{\mathrm{m},0} + \lambda r_{\mathrm{m},0}\,(\mathrm{e}^{(\bar{\psi}-\lambda)t} - 1)/(\bar{\psi} - \lambda);$$

$$r_{\mathrm{m}} = r_{\mathrm{m},0}\,\mathrm{e}^{(\bar{\psi}-\lambda)t}.$$

Values for $\alpha_{m,0}$ and $r_{m,0}$ are known from the Sr–Nd correlation (planetary values) or from Archaean data, for an appropriate time t. Thus values for $\bar{\psi}$ can be calculated (table 2).

It is interesting to compare the values for $\bar{\psi}$ obtained from trace element and from isotopic ratios. For Rb–Sr these values are comparable, but those deduced from isotopic ratios are lower by a factor of 2. This can be explained by the fact that isotopic homogenization is more easily achieved than chemical equilibrium. It is possible to take this effect into account by modifying the equation for α_m (equation (4)) to

$$\left.\begin{aligned} \mathrm{d}\alpha_m/\mathrm{d}t &= \lambda r_m + (\alpha^* - \alpha_m)\,\bar{P}(t);\\ \mathrm{d}r_m/\mathrm{d}t &= (\bar{\psi} - \lambda)\, r_m, \end{aligned}\right\} \tag{8}$$

where $\bar{P}(t)$ describes the isotopic exchange between the system (α_m) and the outside domains (α^*). $\bar{P}(t)$ can reasonably be considered to be constant.

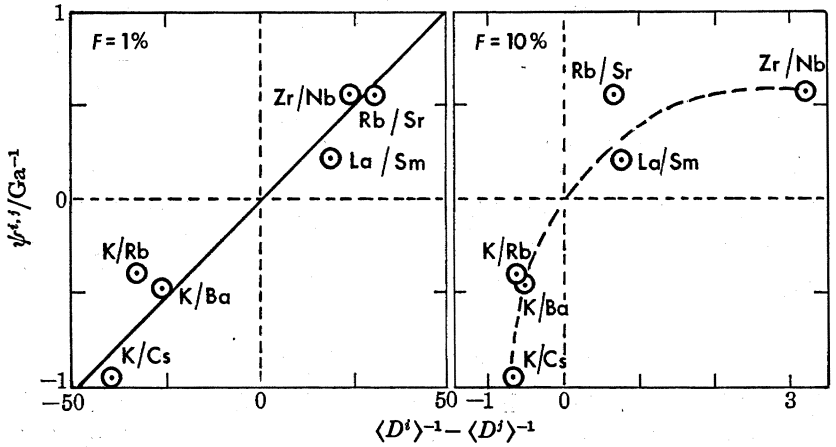

FIGURE 6. Relation between the fractionation factors, $\bar{\psi}^{i,j}$, for pairs of hyg.-elements in the mean mantle and their 'effective' partition coefficients, $\langle D^i\rangle$ and $\langle D^j\rangle$. In this case, all parameters are assumed constant with time. On the right, for a degree of melting $F = 10\%$, no straight correlation is obtained. For $F = 1\%$ (left), the data define a straight line, the slope of which defines a value for $G^{-1}\,\mathrm{d}V/V\mathrm{d}t$ of 2×10^{-11} a^{-1} which corresponds to the time constant of substraction of material from the mantle.

TABLE 2. FRACTIONATION FACTORS, $\bar{\psi}$, FOR THE MEAN MANTLE AS DEDUCED FROM THE EVOLUTION OF ISOTOPIC COMPOSITIONS AND TRACE ELEMENT RATIOS FROM ARCHAEAN TO PRESENT TIMES

	$\bar{\psi}$/Ga^{-1}	
	from isotopes	from chemical ratios
Rb–Sr	0.22	0.546
Sm–Nd	−0.023	−0.083

A mean Archaean Sm/Nd ratio (2.7 Ga ago) of 0.8 has been used. Values deduced from trace element ratios are twice those deduced from isotopic ratios; this is considered to be an indication of the importance of isotopic exchange in the mantle.

The large 'external' domain corresponding to the 'mean' mantle should be defined here. As mentioned previously, the process that fractionates the mean mantle is liquid extraction, which yields basalts. These basalts are reinjected into the mantle along subduction zones but are certainly not redissolved into the 'mean' mantle. This means that chemical exchange between

this basaltic or eclogitic material and the 'mean' mantle does not occur. However, these domains can exchange isotopes more easily.

Evolution curves for the isotopic ratios $^{87}Sr/^{86}Sr$ or $^{143}Nd/^{144}Nd$ can be calculated with the help of the $\overline{\psi}$ values (figure 7). It is interesting that Precambrian isotopic ratios obtained from greenstone belts plot on the planetary evolution curve rather than on the calculated evolution curves with constant fractionation. This implies that $\overline{\psi}$ values are not constant through geological time, and vary with time. Qualitatively, it is already possible to deduce that $\overline{\psi}$ should increase with time.

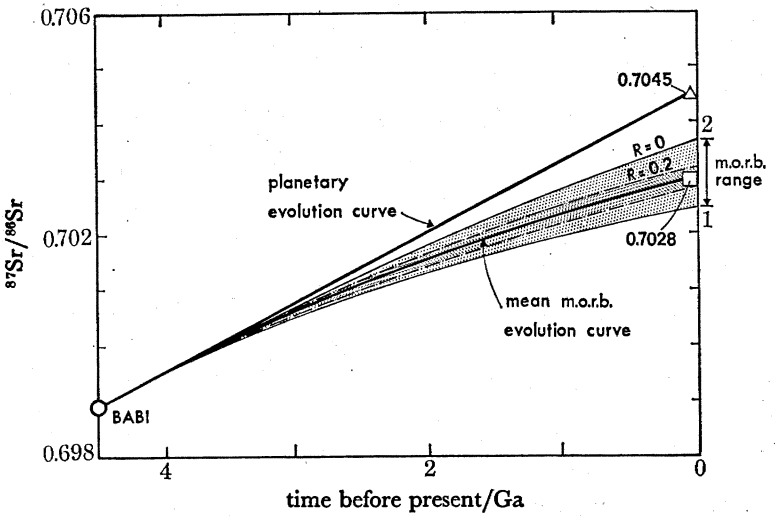

FIGURE 7. Strontium evolution diagram for steady-state behaviour (all parameters constant with time). Starting from $^{87}Sr/^{86}Sr_{BABI}$, 4.55 Ga ago, the mean mantle evolved to yield the present mean value for m.o.r.b. of 0.7028, for a fractionation factor $\overline{\psi}^{Rb-Sr} = 0.15$. In different domains of the mantle, the Sr isotopic composition evolves differently owing to particular fractionation factors. Two possible curves are shown here for $\psi_1^{Rb-Sr} = 0.23 \times 10^{-9}\ a^{-1}$ and $\psi_2^{Rb-Sr} = 0.081 \times 10^{-9}\ a^{-1}$. The present values cover the range of m.o.r.b. data. The effect of mixing is shown: the external curves 1 and 2 are obtained for $R = 0$; for $R = 0.2$, the internal curves are obtained.

Finally, the most difficult part of the problem to quantify is that of the variations of the absolute concentrations of trace elements in the mantle from 3 Ga ago to the present. However, a comparison between trace element concentration in Archaean komatiites and those in recent basalt indicates that the maximum variation is about a factor of 5. This puts a severe constraint on the values for $\overline{\varphi}$. For a purely magmatic fractionation process, and for 10–15% partial melting, then

$$\overline{\varphi} \approx (9 \text{ to } 6)\, W\, dV/V\, dt = \lg 5/(3 \times 10^9),$$

and $dV/V\,dt$ is of the order of $10^{-10}\,a^{-1}$. This is larger than the estimate for recent times, in agreement with the idea that convection was more active in Archaean times than now. With such a rate of convection, half the total mantle could be recycled in 4.5 Ga. If the effective turnover time constant is $10^{-11}\,a^{-1}$, this could indicate that only a part of the lithospheric plate is 'redissolved' in the mantle. This would imply an effective degree of melting, F, of 1%. Indeed, this is understandable if the lower part of the lithospheric plate is redissolved in the mantle, whereas the upper part is not. This lower part of the plate is only depleted by a small degree of melting as shown theoretically by Bottinga (1974) and experimentally by Loubet *et al.* (1975).

Variations around the mean values for m.o.r.b. We may now examine the present-day variations of radiogenic isotopes (Rb–Sr 'mantle isochrons', Nd–Sr correlation, Pb–Pb data) in the light of our continuous model. These variations are assumed to represent variations around the mean mantle values due to variations of two parameters: the fractionation factor, ψ, and the mixing parameter, R. Present-day effects are estimated by integrating (7) for constant values of these parameters. This is illustrated by strontium evolution curves calculated for values of ψ ranging from $\psi_1 = 0.23 \times 10^{-9}\,\mathrm{a}^{-1}$ to $\psi_2 = 0.08 \times 10^{-9}\,\mathrm{a}^{-1}$ (no mixing). For such values, the whole range of Sr isotopic variation in m.o.r.b. can be generated (figure 7). For the same values of ψ, the evolution curves are also represented for $R = 0.2$. This illustrates the extreme efficiency of mixing in narrowing the range of present day Sr isotopic composition.

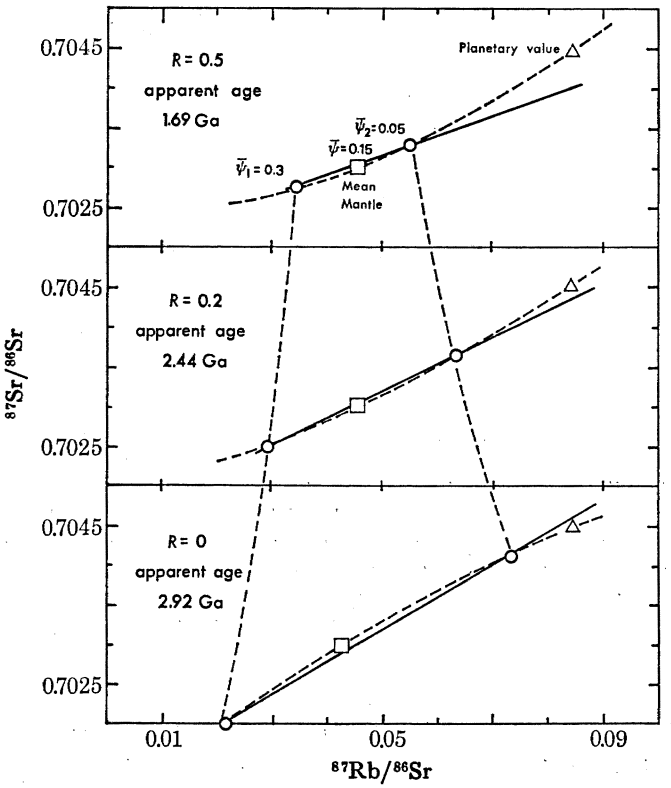

FIGURE 8. $^{87}Sr/^{86}Sr$–$^{87}Rb/^{86}Sr$ diagram for present values. The present mean mantle (squares) and two different domains (circles) obtained for two different fractionation factors, $\psi_1^{Rb\text{-}Sr} = 0.3 \times 10^{-9}\,\mathrm{a}^{-1}$ and $\psi_2^{Rb\text{-}Sr} = 0.05 \times 10^{-9}\,\mathrm{a}^{-1}$, approximately define an isochron of age 2.92 Ga for $R = 0$. The effective trend is shown by the dotted line, which is not significantly different from a straight line. Different values for the mixing parameter, R, narrows the total range of variations and reduces the slope. For $R = 0.5$, an apparent 'mantle isochron' of age 1.69 Ga is obtained, similar to the observed one.

These calculations are also depicted in the ($^{87}Rb/^{86}Sr$–$^{87}Sr/^{86}Sr$) diagram (figure 8). The variations of the fractionation parameter, ψ, around the mean value generate straight lines. In fact, these correlation lines are not straight, but would appear as such within experimental errors. For $R = 0$, this line thus corresponds to a 'mantle isochron' of 'age' 2.9 Ga. Mixing reduces the range of variation, and also modifies the slope of the correlation trend. For values of R of 0.2 and 0.5, 'ages' of 2.44 and 1.69 Ga are obtained. In addition, the apparent 'intercept' of such correlation lines is around $^{87}Sr/^{86}Sr = 0.7015$, similar to that for observed 'mantle isochrons'.

PHILOSOPHICAL TRANSACTIONS OF THE ROYAL SOCIETY A MATHEMATICAL, PHYSICAL & ENGINEERING SCIENCES

As for equation (4), equation (7) can be transformed by considering isotopic exchange. The equation for r remains unchanged, and the equation for α is modified to

$$d\alpha/dt = (\alpha_m - \alpha)\, L(t)\, R(t) + (\alpha_m - \alpha)\, P(t) + \lambda r, \tag{9}$$

where $P(t)$ describes the isotopic exchange between the domain and the mean mantle. Here also, apparent 'mantle isochrons' are obtained, the slope of which correspond to any age (figure 9). This shows clearly that it is possible to generate so called 'mantle isochrons' without discontinuity and catastrophe, but by a continuous process.

In the same way, it is possible to generate a Sr–Nd isotopic correlation similar to the observed one by varying the fractionation parameters ψ^{Sm-Nd} and ψ^{Rb-Sr} such that $\psi^{Sm-Nd}/\psi^{Rb-Sr} = -0.15$ (figure 10). As discussed by Allègre *et al.* (1979*a*), such a relation between the Sm, Nd, Rb, and Sr partition coefficients argues in favour of a magmatic solid–liquid fractionation process.

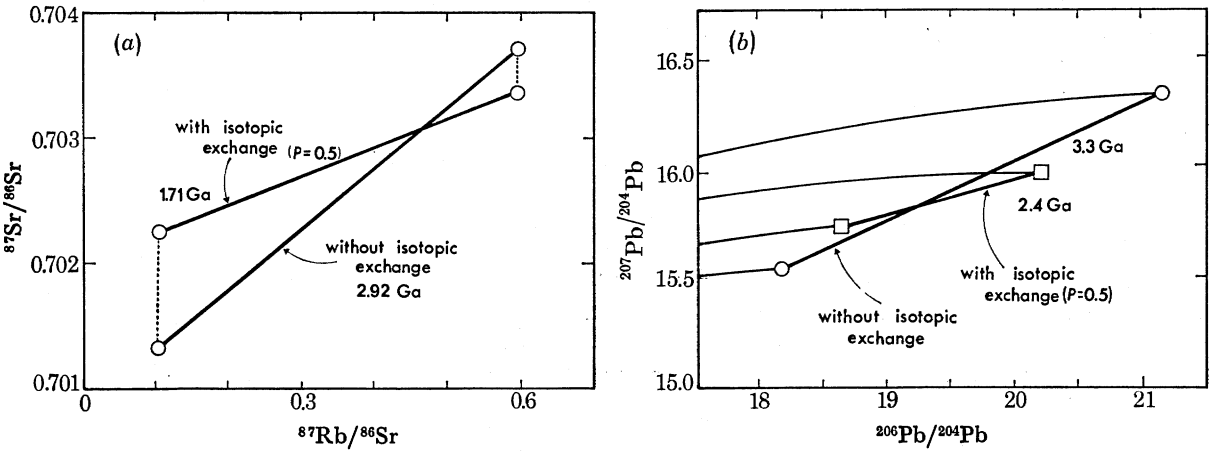

FIGURE 9. Effect of the isotopic exchange term on the apparent 'mantle isochrons'. Part (*a*) corresponds to figure 8 ($R = 0$): isotopic exchange significantly lowers the slope of the apparent isochron. Part (*b*) corresponds to figure 11: lower slopes are obtained, but the steady-state model does not describe all Pb isotopic data.

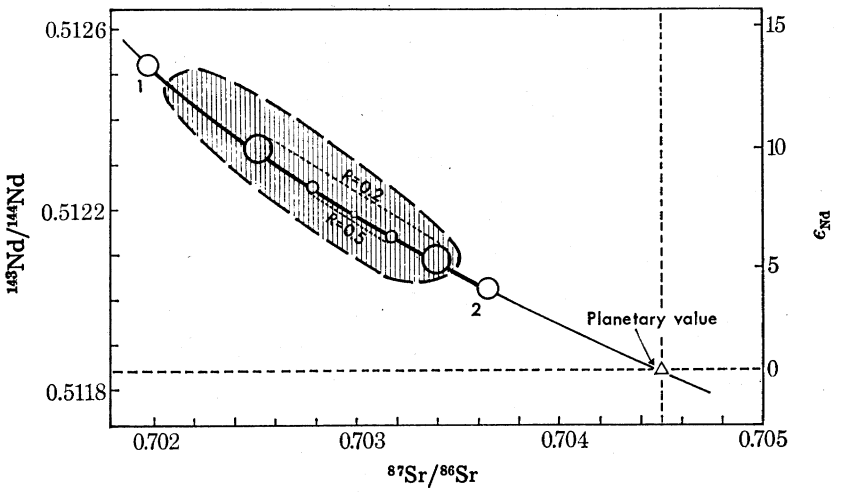

FIGURE 10. Sr–Nd correlation. If the fractionation factors follow the relation $\psi^{Sm-Nd}/\psi^{Rb-Sr} = -0.15$, a correlation line similar to the observed one for m.o.r.b. (see figure 1) is obtained in the steady-state model. For different values of R, the range of values is narrowed but the correlation remains similar.

Similar calculations have been made for lead isotopes. In a Pb–Pb isotope diagram, it is possible to generate J-type lead and straight correlations by varying ψ^{U-Pb}. However, whatever the variations in ψ^{U-Pb} and R, these straight lines yield apparent Pb–Pb isochrons of 'age' older than 2.6 Ga (figure 11). It appears impossible to generate Pb–Pb isochrons 1.3–2 Ga old by this method. Lower slopes can be obtained on the Pb–Pb diagram by considering the effects of the isotopic exchange (equation (9), figure 9). However, the whole domain of Pb–Pb observed data cannot be mapped by constant parameter models. As we have noted, this could reveal complex U–Pb fractionation processes, time-related fractionation or an ancient Pb isotope heterogeneity.

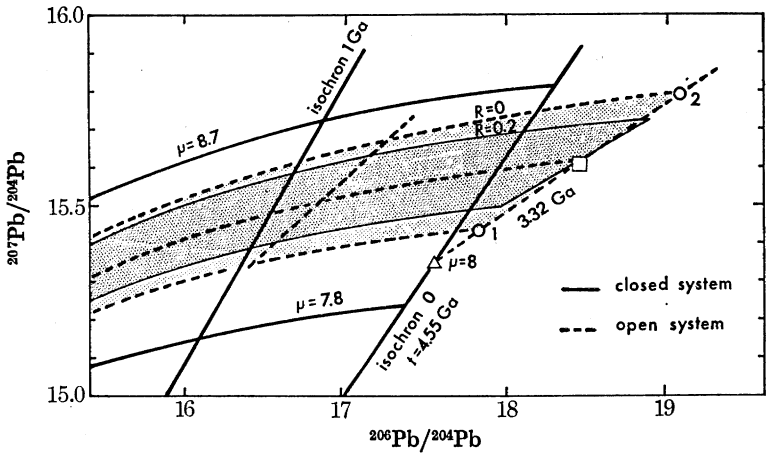

FIGURE 11. $^{207}Pb/^{204}Pb$–$^{206}Pb/^{204}Pb$ for the steady-state model. For different fractionation factors, ψ^{U-Pb}, and mixing factors, R, it is indeed possible to obtain apparent straight lines, but they yield apparent ages not younger than 2.5 Ga. This indicates that the fractionation and mixing factors are more complex than in the steady-state model.

The model can also be applied to the present-day variations of hyg.-elements. The present variations, as well as the correlations between elemental and isotopic ratios, can be calculated. Here we shall consider only the correlations between two hyg.-element ratios.

We shall first neglect the mixing process, and consider only the variations of the ratios resulting from various degrees of fractionation. Then, to a first approximation, (6) can be integrated to give

$$\lg r^{i,j} = \lg r_0^{i,j} + \psi^{i,j} t;$$

$$\lg r^{k,l} = \lg r_0^{k,l} + \psi^{k,l} t.$$

By eliminating the t, and if

$$\frac{\psi^{i,j}}{\psi^{k,l}} = \frac{1/\bar{D}^i - 1/\bar{D}^j}{1/\bar{D}^k - 1/\bar{D}^l} = \text{constant},$$

then, for different $\psi^{i,j}$, one obtains a straight line in a ($\lg r^{i,j}$–$\lg r^{k,l}$) diagram. For hyg.-elements the above condition is reasonable (Allègre *et al.* 1979*a*) and our model explains adequately the correlation of figure 3*b*.

(*c*) *Variation of the parameters with time*

The above analysis reveals that it is not possible to describe all of the observed features by a constant parameter model. Precambrian Nd and Sr isotopic compositions are not obtained by reversing the constant fractionation process resulting in present m.o.r.b. type values; neither can

Pb isotope systematics be satisfied by such a model. Thus it is necessary to examine the effects of the parameters themselves with time.

Mean mantle. Following MacKenzie & Weiss (1975) and O'Nions *et al.* (this symposium), we assume that the convecting activity has decreased with time. Therefore, $\mathrm{d}V/\mathrm{d}t$ has probably decayed with time. If convection became restricted to the upper mantle, V also decayed with time. The degree of partial melting which has affected the mantle was probably higher during the Precambrian as attested by komatiites. Thus the factor $\{(G\langle D\rangle)^{-1}-1\}$ has increased with time. We shall assume simple exponential variations of these parameters:

$$\bar{\varphi}^*(t) = \bar{\varphi}_0^* \, \mathrm{e}^{(1/\tau_2 - 1/\tau_1)t},$$

where τ_1 and τ_2 are the time constant of the variations of $\{(G\langle D\rangle)^{-1}-1\}$ and $V\mathrm{d}V/\mathrm{d}t$ respectively. One expects that $\tau_2 < \tau_1$, which implies that $\bar{\varphi}^*$ increased with time.

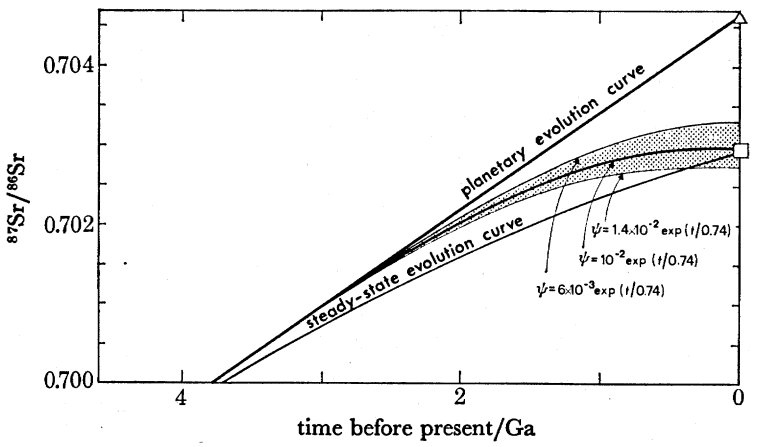

FIGURE 12. Evolution diagram for Sr for variable fractionation factors. A time constant of 0.74 Ga has been used in this diagram. The Sr evolution paths are more curved than for the steady state model. Thus, the model satisfies both the Precambrian data and the present m.o.r.b. data. A time constant of 2–3 Ga is probably more reasonable (see text).

As a first approximation, we shall also describe the variation of $\bar{\psi}$, the fractionation function for a ratio, as exponential with time: $\bar{\psi} = \bar{\psi}_0 \mathrm{e}^{t/\tau}$; τ can be estimated from the evolution of $^{87}Sr/^{86}Sr$ and $^{143}Nd/^{144}Nd$, to satisfy on a single evolution curve the Precambrian data and present m.o.r.b. values.

Equations (3) and (4) can be integrated to give

$$r_{\mathrm{m}}^{i,j} = r_{\mathrm{m},0}^{i,j} \exp[\tau\bar{\psi}_0\{\mathrm{e}^{t/\tau}-1\}] \quad \text{for trace element ratios;}$$

$$r_{\mathrm{m}} = r_{\mathrm{m},0} \exp[\tau\bar{\psi}_0\{\mathrm{e}^{t/\tau}-1\} - \lambda t] \quad \text{for parent: daughter ratios;}$$

$$\alpha_{\mathrm{m}} = \alpha_{\mathrm{m},0} + \lambda r_{\mathrm{m},0} \int_0^t \exp[\tau\bar{\psi}_0\{\mathrm{e}^{t/\tau}-1\} - \lambda\theta]\,\mathrm{d}\theta \quad \text{for daughter isotopic ratios.}$$

The best fit of the data corresponds to a time constant of 0.74 Ga from both Sr and Nd constraints (figure 12). Secondly, it is then possible to estimate values for $\bar{\psi}_0$ as deduced from the variations of the hyg.-element ratios. These values are given in table 3. A problem then arises, identical to that for the steady state models: the time constant deduced from the $^{87}Sr/^{86}Sr$ evolution results in a much too large variation of the elemental Rb/Sr ratio. Again, this is consistent with the idea that isotopic exchange is much easier than chemical homogenization.

Being thermally activated and related to mixing, isotopic exchange decreases with time. We assume again that $\bar{P}(t)$ decreases exponentially with time. The time constant, τ, deduced from the isotopic data is thus too small to describe the chemical fractionation process. A more reasonable estimate of τ of 2–3 Ga gives new estimates of the constants $\overline{\psi}_0$ which are given in table 3.

TABLE 3. FRACTIONATION FACTORS FOR HYG. ELEMENT RATIOS

	$\overline{\psi}_0$/Ga	
	$\tau = 0.74$ Ga	$\tau = 2$ Ga
K/Ba	−0.0039	−0.09
K/Cs	−0.0078	−0.18
K/Rb	0.0032	−0.075
Rb/Sr	0.0044	0.10
Ti/Y	−0.00044	−0.0103
Ti/Zr	0	0
Zr/Nb	0.0043	0.101
Zr/Y	0	0
(La/Sm)†	0.0015	0.034

The mean fractionation factors $\overline{\psi} = \overline{\psi}_0 e^{t/\tau}$ have been calculated as in table 1, for two time constants $\tau = 0.74$ Ga and $\tau = 2$ Ga. Comparison of the fractionation factor $\overline{\psi}^{Rb-Sr}$ deduced from $^{87}Sr/^{86}Sr$ evolution and Rb/Sr evolution indicates that isotopic exchange has to be considered, and that the time constant is rather long ($\tau = 2$–3 Ga).

† Normalized to chondrites.

It is thus possible to solve the difficulties encountered in our steady state models of the mean mantle evolution by taking into account the decrease with time of the thermal activity of the mantle. However, a time-dependent fractionation model does not eliminate the 'uranium-lead paradox'. We shall return to this aspect later.

Mantle domains. For mantle domains, both ψ and R vary with time: ψ probably increases with time, and R, which is related to the stirring efficiency, decreases with time, starting from a value close to unity. As a consequence, the isotopic exchange efficiency decreases with time.

It is quite easy to match the observed Nd–Sr isotopic correlation with such a model. Reasonable slopes can be also obtained for the Rb–Sr 'mantle isochrons' and the Pb–Pb trends. In order to obtain the present dispersion of the $^{206}Pb/^{204}Pb$ and $^{207}Pb/^{204}Pb$ ratios, and for R

TABLE 4. FRACTIONATION (ψ) AND MIXING (R) FACTORS AND APPARENT AGE FOR THE $^{207}Pb/^{204}Pb$–$^{206}Pb/^{204}Pb$ DIAGRAM

	parameters	apparent age/Ga
steady-state	$R = 0; \psi = \psi_0$	3.32
	$R = 0.2; \psi = \psi_0$	3.04
	$R = 0.5; \psi = \psi_0$	2.54
variable with time	$R = \exp(-0.35t); \psi = \psi_0$	1.64
	$R = 0.2\exp(-0.15t); \psi = \psi_0$	3.17
	$\psi = \psi_0 \exp(0.15t); R = 0$	3.28
	$\psi = \psi_0 \exp(-0.15t); R = 0$	3.39
	$\psi = \psi_0 \exp(0.35t); R = 0$	3.08

The upper part corresponds to the steady-state model where the parameters are maintained constant with time. The lower part is a non-steady-state model. First ψ is maintained constant and R varies with time. Different values for ψ yield an apparent 'mantle isochron', the age of which is listed. Then R is maintained constant ($R = 0$) and ψ varies with time. The 'isochron' is obtained for different ψ_0 values.

PHILOSOPHICAL TRANSACTIONS OF THE ROYAL SOCIETY A MATHEMATICAL, PHYSICAL & ENGINEERING SCIENCES

decreasing from unity at 4.55 Ga to 0.2 today, we have to consider a range of ψ values from -0.01 to -1.0 (table 4). This would imply larger differences between the different régimes of magmatic fractionation than previously assumed. It should, however, be noted that the problem is poorly constrained. Whereas the present-day variations for both isotopes and trace elements are known, they are not in the past and especially during the Archaean. Such an approach only describes the *range of variations* of the present chemical and isotopic data. It is desirable to describe also the *distribution* of these data. It should be possible to achieve this by formulating the problem as a *stochastic* rather than a *deterministic* one.

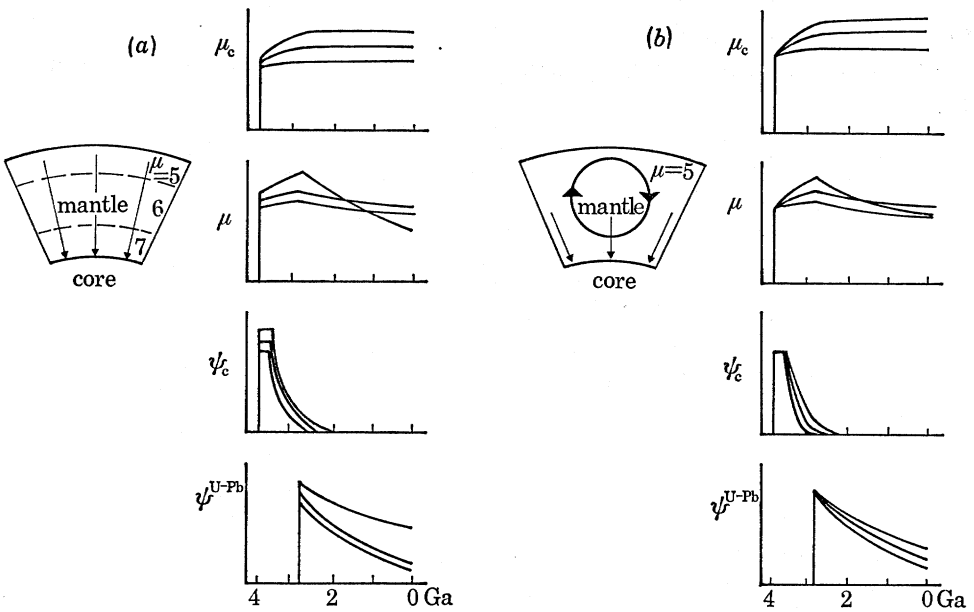

FIGURE 13. Schematic diagram showing possible effects of core formation on U–Pb fractionation. We envisage that some Pb was segregated in the core during a limited period (200 Ga) after Earth formation. Processes connected with formation of the continental crust only started to efficiently fractionate U and Pb some time after and has continued until the present day (Allègre & Brévart, to be published). $\mu = {}^{238}U/{}^{204}Pb$; μ_c, evolution of μ due to core formation only; ψ_c, U–Pb fractionation factors for different domains due to core formation; ψ^{U-Pb}, fractionation factor due to surface fractionation. For (*a*), mixing in the mantle was not effective enough to homogenize U and Pb and an 'initial' heterogeneity is created by the core formation. For (*b*), mixing results in a homogeneous U/Pb ratio in the mantle. Subsequent U/Pb fractionation due to surface effects may result in complex evolution of μ in the different domains.

(*d*) *The 'lead paradox': evidence for core–mantle interaction?*

The 'lead paradox'. The Nd–Sr–Pb correlations in m.o.r.b. from North Atlantic indicate that the planetary values for Pb isotopes corresponding to $^{87}Sr/^{86}Sr = 0.7045$ are $^{206}Pb/^{204}Pb = 21.0$ and $^{207}Pb/^{204}Pb = 15.7$. This is far inside the classical field for J-type lead isotopic compositions.

Alkali basalts from the Japan sea (Okidogo–Takashima) bear planetary values for Nd and Sr isotopic ratios, and Hf/Th and Ta/Th element ratios. However, their Pb isotopic ratio $^{206}Pb/^{204}Pb$ is equal to 17.8, and correspond to the classical closed system value (using an age of 4.55 Ga, the new uranium decay constants and the initial Pb isotopic composition of the Canyon Diablo troilite of Tatsumoto *et al.* (1973) and Allègre *et al.* (1979*b*)). It seems thus that two extreme 'planetary' values for Pb isotopes may coexist.

As pointed out by Allègre (1969), the U–Pb fractionation in the Earth's mantle is paradoxical: while U is more magmatophile than Pb, the U/Pb ratio of the mantle increases with time. In

addition the distribution of the U–Pb integrated fractionation as measured by Pb isotopes is the reverse of that of U–Pb distribution.

As mentioned previously, while the U–Pb–Pb systems are chemically identical, compared with the Rb–Sr and Sm–Nd systems, they do not define straight correlation lines but rather map into a two-dimensional domain in the Pb–Pb isotope diagram.

Quantitative approach. To interpret the above facts, we assume that the early mantle experienced core formation. Because of the probable presence of sulphur in the core (Murthy & Hall 1970) and of the chalcophile character of lead, some lead enters the core, but uranium and thorium do not. This is clearly illustrated by the study of the U–Th–Pb systems in iron meteorites. This process results in an increase of the value of $^{238}U/^{204}Pb = \mu$ from 0.1 in primitive chondrites to apparently about 7–8 in the present Earth mantle. Some aspects of this model are shown in figure 13.

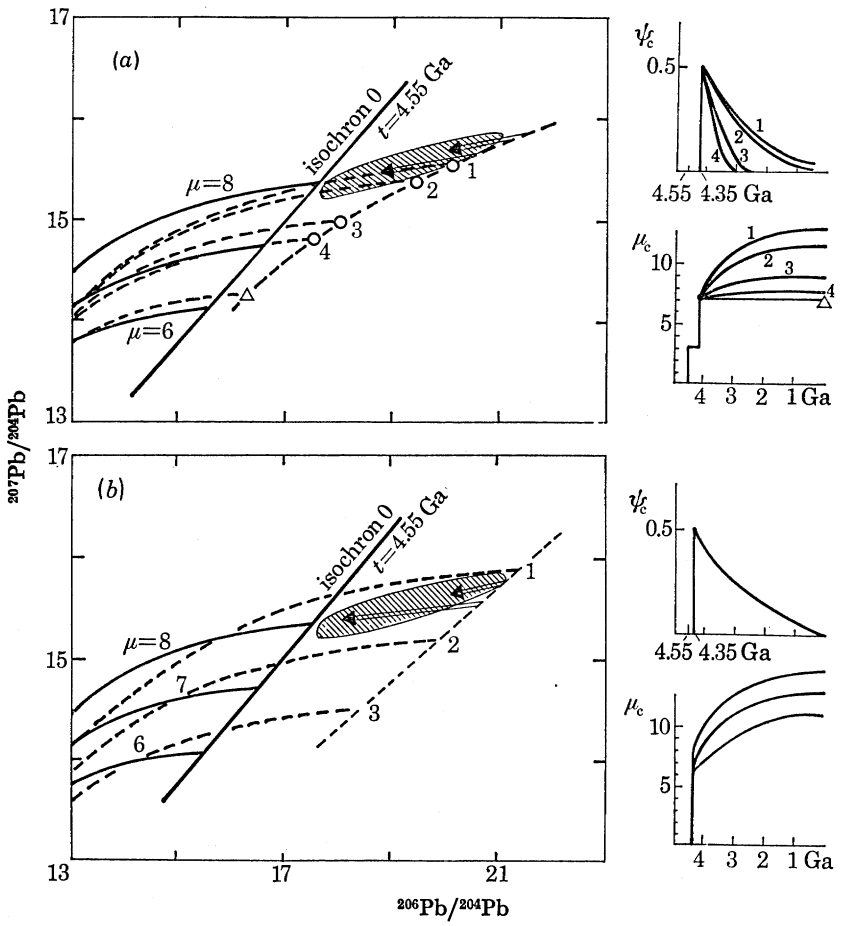

FIGURE 14. $^{207}Pb/^{204}Pb$–$^{206}Pb/^{204}Pb$ diagram showing the effect of U–Pb core fractionation on present lead isotopic composition. In both (*a*) and (*b*), closed system evolution curves and geochrons as well as the domain for m.o.r.b. are shown for reference (heavy lines and hatched area respectively). For (*a*), we have taken that μ_c ($^{238}U/^{204}Pb$ due to core formation) to be homogeneous and equal to 3 until 4.35 Ga ago. Then fractionation due to core formation (ψ_c) was suddenly effective and decreased with different time constants in different mantle domains (from 0.3 Ga for point 4 to 1.2 Ga for point 1). Fractionation to the surface is described by the large arrows. For (*b*), ψ_c has been inequally efficient in different mantle domains 4.35 Ga ago, but was subsequently similar everywhere (time constant 1.2 Ga). Points 1 to 3 thus represent domains with different initial values for μ (from 6 to 8). Such models are only two possible cases exemplifying the effects of core formation.

To obtain the two point 'undifferentiated planetary' line represented by the Takashima alkali basalt and the extreme North Atlantic m.o.r.b., it is necessary that differentiation occurred very early in Earth history. Some domains of the mantle may have been more strongly affected by core formation than others. This could be imagined as a zonation with depth, with lead isotopic compositions subsequently following different evolutionary paths. During later mantle fractionation processes U is more incompatible than Pb; therefore $\overline{\psi}^{\mathrm{U-Pb}}$ is positive and the Pb isotopic composition in the residual mantle is of type B relative to the 'planetary' evolution lines.

We introduce a fractionation factor $\overline{\psi}_{\mathrm{c}}$ to the core such that $\overline{\psi}_{\mathrm{c}} = \overline{\psi}_{0,\mathrm{c}}\, \mathrm{e}^{-t/\tau_3}$. The mathematical expressions (8) are transformed to

$$\mathrm{d}\alpha_{\mathrm{m}}/\mathrm{d}t = \lambda r + (\alpha^* - \alpha_{\mathrm{m}})\, \bar{P}(t)$$

and

$$\mathrm{d}r_{\mathrm{m}}/\mathrm{d}t = (\overline{\psi}_{\mathrm{c}} + \overline{\psi} - \lambda)\, r_{\mathrm{m}}.$$

Within the frame of the above hypothesis, which can be described by different time constants $\tau = 2\,\mathrm{Ga}$ and $\tau_3 = 0.5\,\mathrm{Ga}$, it is possible to describe the U–Pb data, and in particular to solve the U–Pb fractionation paradox. For the domains, equations (9) are transformed into

$$\mathrm{d}\alpha/\mathrm{d}t = (\alpha_{\mathrm{m}} - \alpha)\, L(t)\, R(t) + (\alpha^* - \alpha)\, P(t) + \lambda r$$

and

$$\mathrm{d}r/\mathrm{d}t = (r_{\mathrm{m}} - r)\, L(t)\, R(t) + (\psi_{\mathrm{c}} + \psi - \lambda)\, r.$$

It is possible to obtain a two-dimensional mapping in the Pb–Pb diagram by such a model (figure 14).

Conclusions

1. The correlations between mantle chemical and isotopic ratios and, in particular, the 'mantle' isochrons and Sr–Nd correlations can be modelled easily by a continuous process. The discrepancies which are observed between the Sm–Nd, Rb–Sr and Pb–Pb 'apparent ages' of the mantle isochrons can be more easily understood in the framework of a continuous model.

2. The mantle chemical heterogeneity cannot be created by mixing with continental crust material since continental crust is the chemical complement of the mantle relative to the planetary values. We have divided the chemical fractionation effects in the mantle into a mean fractionation and domain fractionations. Mean variation is created by continuous extraction processes which mainly involve solid–liquid partitioning and result in an evolution which differs from the planetary evolution. Local heterogeneities can be explained by mixing of different mantle domains which have different extraction parameters. Subducted sediments may participate in this domain heterogeneity, but this seems on present evidence to be a minor phenomenon.

3. A quantitative model, based on a dual estimation of the mean and domain evolutions, reveals the following features.

(*a*) Isotopic exchanges during mantle mixing have to be considered.

(*b*) The fractionation and mixing parameters have varied with time. A time constant for this variation (essentially that for convection) of about 2 Ga appears reasonable. However, many features are correctly explained by a steady-state model: this is a consequence of the balance between increased efficiency of mixing and of fractionation due to an increased efficiency of convection.

PHILOSOPHICAL TRANSACTIONS OF THE ROYAL SOCIETY A MATHEMATICAL, PHYSICAL & ENGINEERING SCIENCES

(*c*) The data, and in particular the evolution of trace element concentrations, are better explained if the oceanic crust material becomes isolated from the mantle.

(*d*) The U–Pb data require a complex fractionation process. They are best explained by an early episode of core formation, in which Pb is fractionated into the core as sulphides, but where the core formation extended over the first few hundred million years of Earth history. A time constant for core fractionation of about 0.2 Ga could fit the data. Thus, core formation is not a sudden process in this model.

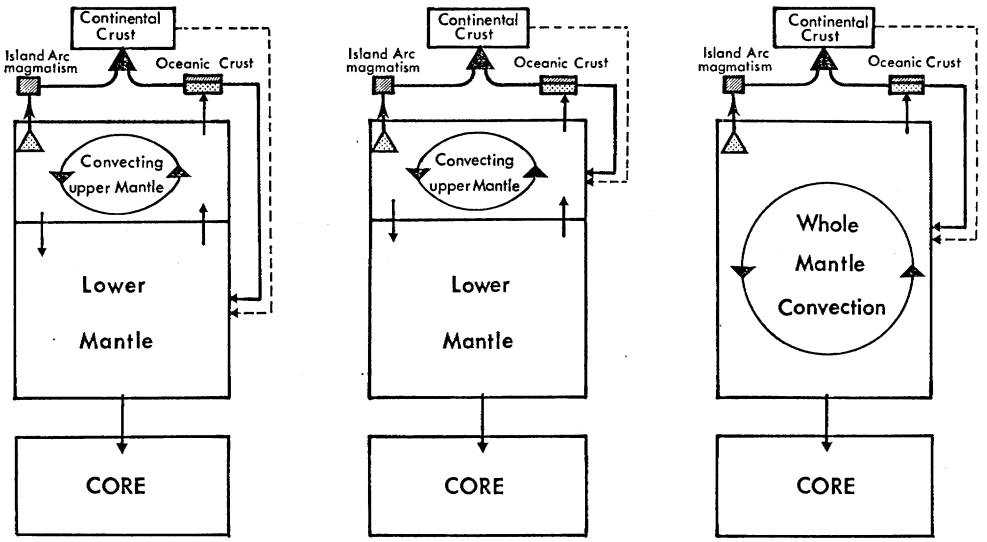

FIGURE 15. Schematic diagram showing some possible box models for mantle chemical fractionation. There is a distinction between fractionation into the core (U–Pb fractionation) and to the surface (island arcs – oceanic crust – continental crust). Evolution in the mantle depends on whether convection affects the whole mantle (right) or only the upper mantle. In the latter case, exchanges between the lower and upper mantle must be considered. Crustal material (oceanic or continental) may be reinjected into the mantle along subduction zones and may be directed towards the upper mantle (middle) or the lower mantle (left).

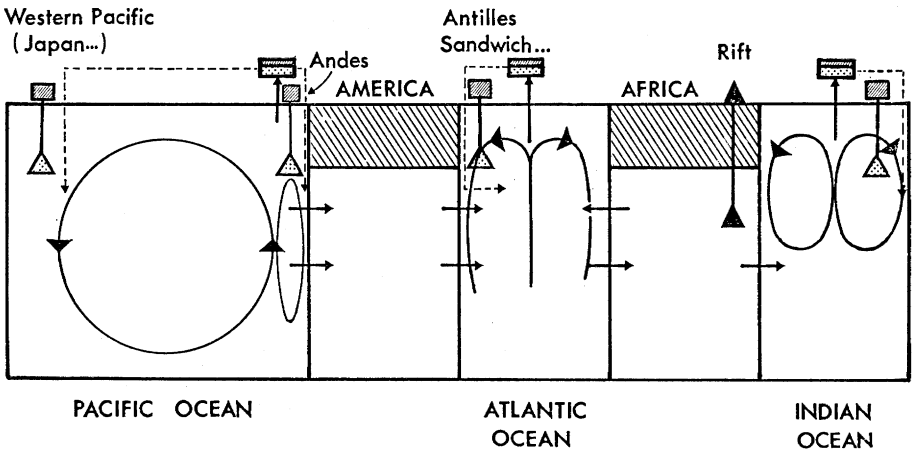

FIGURE 16. Schematic diagram describing a lateral box model for mantle exchanges. The symbols are the same as for figure 15. It is important to consider the possible exchange of mantle material from the subcontinental mantle to the oceanic mantle: this may have occurred in the Atlantic Ocean, whereas the sub-Pacific mantle may have remained essentially oceanic during several hundred million years.

PHILOSOPHICAL TRANSACTIONS OF THE ROYAL SOCIETY A MATHEMATICAL, PHYSICAL & ENGINEERING SCIENCES

(*e*) The heterogeneity of those elements that did not enter into the core is not a consequence of heterogeneous accretion. Rather it results from continuous extraction of these elements out of the mantle and into the continental crust. This process is intimately linked with mantle convection. Such a dual process fits heterogeneity of lead isotopes associated with homogeneity of strontium and neodymium isotopes in Precambrian materials.

Unsolved problems

1. At the moment, the problem of whether convection affects the whole mantle or is restricted to the upper mantle is not solved.

2. The dilemma of the relation between m.o.r.b. and ocean island basalt sources is not solved.

3. There are several indications of the need to study mantle heterogeneity on a regional rather than a whole Earth scale. Considerations such as those depicted by the regional box model schematized in figure 16 can be a step towards a better understanding of these heterogeneities. It should however, be emphasized that the transfer parameters as well as the boxes themselves can vary with time. We think that a regional approach could help in understanding the m.o.r.b.–oceanic island basalt problem itself.

We acknowledge the 'Cyclope'† colleagues for stimulating scientific exchange on those problems and especially for their hot discussion on 'mantle isochrons'. A. Provost and M. Condomines corrected the manuscript with great care. J. Tarney made a number of useful suggestions and improvements.

References (Allègre *et al.*)

Allègre, C. J. 1969 *Earth planet. Sci. Lett.* **5**, 261–269.
Allègre, C. J. & Bottinga, Y. 1974 *Nature, Lond.* **252**, 31–32.
Allègre, C. J. & Minster, J.-F. 1978 *Earth planet. Sci. Lett.* **38**, 1–25.
Allègre, C. J., Ben Othman, D., Polvé, M. & Richard, P. 1979*a* *Phys. Earth. planet. Inter.* **19**, 293–306.
Allègre, C. J., Manhes, G., Richard, P., Rousseau, D. & Shimizu, N. 1978 Presented at 6ème Réunion Annuelle des Sciences de la Terre, Orsay.
Allègre, C. J., Montigny, R. & Bottinga, Y. 1973 *Bull. Soc. géol. Fr.* (7) **15**, 461–477.
Allègre, C. J., Richard, P., Treuil, M., Joron, J.-L. & Tatsumoto, M. 1979*b* *Eos, Wash.* **60**, 413.
Allègre, C. J., Treuil, M., Minster, J.-F., Minster, B. & Albarède, F. 1977 *Contr. Miner. Petr.* **60**, 57–75.
Armstrong, R. L. 1968 *Rev. Geophys.* **6**, 175–199.
Basu, A. & Murthy, V. R. 1977 *Earth planet. Sci. Lett.* **35**, 239–246.
Beswick, A. E. 1976 *Geochim. cosmochim. Acta* **40**, 1167–1183.
Beswick, A. E. & Carmichael, I. S. E. 1978 *Contr. Miner. Petr.* **67**, 317–330.
Bottinga, Y. 1974 *Tectonophysics* **21**, 15–38.
Boudier, F. 1976 Doctoral thesis, Université de Nantes.
Boulos, M. S. & Manuel, O. K. 1971 *Science, N.Y.* **174**, 1334–1336.
Brooks, C. & Hart, S. R. 1978 *Nature, Lond.* **271**, 220–223.
Brooks, C., Hart, S. R., Hofmann, A. & James, D. E. 1976 *Earth planet. Sci. Lett.* **32**, 51–61.
Brunn, J. H. 1960 *Revue Géogr. phys. Geol. dyn.* **3**, 115–132.
Carlson, R. W., MacDougall, J. D. & Lugmair, G. W. 1978 *Geophys. Res. Lett.* **5**, 229–232.
Coleman, R. G. 1971 *J. geophys, Res.* **76**, 1212–1222.
Dasch, E. J., Hedge, C. E. & Dymond, J. 1973 *Earth planet. Sci. Lett.* **19**, 177–183.
DePaolo, D. J. & Wasserburg, G. J. 1976 *Geophys. Res. Lett.* **3**, 743–746.
Dupré, B. & Allègre, C. J. 1980 *Nature, Lond.* (Submitted.)
Dupré, B., Hamelin, B. & Allègre, C. J. 1979 *Eos, Wash.* **60**, 414.

† 'Cyclope' consists of C. Brooks, S. R. Hart, G. W. Wetherill, F. R. Tera, P. Eberhart, V. R. Murthy, W. Van Schmus and C. J. Allègre.

Eggler, D. H. 1975 *Carnegie Instn Wash. Yb.* **74**, 468–474.
Engel, A. E. S. & Engel, C. G. 1964 *Science, N.Y.* **144**, 1330–1333.
Erlank, A. J. & Rickard, R. S. 1977 In *Second International Kimberlite Conference, extended abstracts.*
Faure, D. & Elliot, D. H. 1971 *Br. Antarctic Surv. Bull.* **25**, 23.
Faure, G. & Powell, J. L. 1972 *Strontium isotope geology.* (188 pages.) New York: Springer-Verlag.
Frey, F. A. 1969 *Geochim. cosmochim. Acta* **33**, 1429–1447.
Frey, F. A. & Green, D. H. 1974 *Geochim. cosmochim. Acta* **38**, 1023–1059.
Frey, F. A. & Prinz, M. 1978 *Earth planet. Sci. Lett.* **38**, 129–176.
Gast, P. W. 1960 *J. geophys. Res.* **65**, 1287–1297.
Gast, P. W. 1968 *Geochim. cosmochim. Acta* **32**, 1057–1086.
Gast, P. W., Tilton, G. R. & Hedge, C. E. 1964 *Science, N.Y.* **145**, 1181–1185.
Green, D. H. 1971 *Phil. Trans. R. Soc. Lond.* A **268**, 707–725.
Griffin, W. L. & Murthy, V. R. 1969 *Geochim. cosmochim. Acta* **33**, 1389–1414.
Gurney, J. J., Jakob, W. R. O. & Dawson, J. B. 1977 In *Second International Kimberlite Conference, extended abstracts.*
Hamilton, P. J., O'Nions, R. K. & Evensen, N. M. 1977 *Earth planet. Sci. Lett.* **36**, 263–268.
Hart, S. R. 1969 *Earth planet. Sci. Lett.* **6**, 295–303.
Hart, S. R. 1971 *Phil. Trans. R. Soc. Lond.* A **268**, 573–587.
Hart, S. R. & Allègre, C. J. 1979 *Bowen Memorial Volume.* Princeton University Press.
Hart, S. R. & Brooks, C. 1977 *Contr. Miner. Petr.* **61**, 109–128.
Hart, S. R., Brooks, C., Krogh, T. E., Davis, G. L. & Nava, D. 1970 *Earth planet. Sci. Lett.* **10**, 17–28.
Hart, S. R., Erlank, A. J. & Kable, E. J. 1974 *Contr. Miner. Petr.* **44**, 219–230.
Hart, S. R., Schilling, J. G. & Powell, J. L. 1973 *Nature, phys. Sci.* **246**, 104–107.
Hedge, C. E. & Walthall, F. G. 1963 *Science, N.Y.* **140**, 1214–1217.
Hofmann, A. W. & Hart, S. R. 1975 *Carnegie Instn Wash. Yb.* **74**, 195–210.
Hofmann, A. W. & Hart, S. R. 1978 *Earth planet. Sci. Lett.* **38**, 44–62.
Hurley, P. M., Hughes, H., Faure, G., Fairbairn, H. W. & Pinson, W. H. 1962 *J. geophys. Res.* **67**, 5315–5334.
Joron, J. L. & Treuil, M. 1979 (In preparation.)
Kornprobst, M. J. 1969 *Contr. Miner. Petr.* **23**, 283–322.
Kramers, J. D. 1979 *Earth planet. Sci. Lett.* **42**, 58–70.
Langmuir, C. H., Vocke, R. D. J., Hanson, G. H. & Hart, S. R. 1978 *Earth planet. Sci. Lett.* **37**, 380–392.
Leggo, P. J. & Hutchison, R. 1968 *Earth planet. Sci. Lett.* **5**, 71–75.
Le Pichon, X., Francheteau, J. & Bonnin, J. 1973 *Plate tectonics.* (300 pages.) Amsterdam: Elsevier.
Loubet, M., Shimizu, N. & Allègre, C. J. 1975 *Contr. Miner. Petr.* **53**, 1–12.
Lovering, J. F. & Tatsumoto, M. 1968 *Earth planet. Sci. Lett.* **4**, 350–356.
MacKenzie, D. P. & Weiss, N. O. 1975 *Geophys. J.* **42**, 131–174.
MacKenzie, D. P., Roberts, J. M. & Weiss, N. O. 1974 *J. Fluid Mech.* **62**, 465–538.
Manhes, G., Allègre, C. J., Dupré, B. & Hamelin, B. 1980 *Earth planet. Sci. Lett.* (In the press.)
Menzies, M. M. & Murthy, V. R. 1978 *Earth planet. Sci. Lett.* **38**, 346–354.
Minster, J.-F. & Allègre, C. J. 1978 *Contr. Miner. Petr.* **68**, 37–52.
Murthy, V. R. & Hall, H. T. 1970 *Phys. Earth planet. Inter.* **2**, 276–282.
O'Hara, M. J. 1968 *Earth Sci. Rev.* **4**, 69–133.
O'Nions, R. K. & Pankhurst, R. J. 1978 *Earth planet. Sci. Lett.* **22**, 328–338.
O'Nions, R. K., Evensen, N. M., Hamilton, P. J. & Carter, S. R. 1978 *Phil. Trans. R. Soc. Lond.* A **288**, 547–559.
O'Nions, R. K., Hamilton, P. J. & Evensen, N. M. 1977 *Earth planet. Sci. Lett.* **34**, 13–22.
Polvé, M. & Allègre, C. J. 1980 *Earth planet. Sci. Lett.* (In the press.)
Richard, P. & Allègre, C. J. 1980 *Earth planet. Sci. Lett.* (In the press.)
Richard, P., Shimizu, N. & Allègre, C. J. 1976 *Earth planet. Sci. Lett.* **31**, 269–278.
Richter, F. M. 1973 *J. geophys. Res.* **78**, 8735–8745.
Richter, F. M. & MacKenzie, D. P. 1978 *J. Geophys.* **44**, 441–471.
Richter, F. M. & Ribe, N. 1979 *Earth planet. Sci. Lett.* **43**, 212–222.
Rison, W. & Kyser, K. 1977 *Eos, Wash.* **58**, 537.
Schilling, J. G. 1973 *Nature, Lond.* **242**, 565–571.
Shimizu, N. 1975 *Earth planet. Sci. Lett.* **25**, 26–32.
Shimizu, N. & Allègre, C. J. 1978 *Contr. Miner. Petr.* **67**, 41–50.
Stettler, A. & Allègre, C. J. 1978 *Earth planet. Sci. Lett.* **38**, 364–372.
Stettler, A. & Allègre, C. J. 1979 *Earth planet. Sci. Lett.* (In the press.)
Stueber, A. M. & Ikramuddin, R. 1974 *Geochim. cosmochim. Acta* **38**, 207–216.
Sun, S. S. & Hanson, G. N. 1975*a* *Geology* **3**, 297–302.
Sun, S. S. & Hanson, G. N. 1975*b* *Contr. Miner. Petr.* **52**, 77–106.
Sun, S. S. & Nesbitt, R. W. 1977 *Earth planet. Sci. Lett.* **35**, 429–448.
Sun, S. S., Tatsumoto, M. & Schilling, J. G. 1975 *Science, N.Y.* **190**, 143–147.
Tatsumoto, M. 1966 *Science, N.Y.* **153**, 1094–1101.
Tatsumoto, M. 1978 *Earth planet. Sci. Lett.* **38**, 63–87.

PHILOSOPHICAL TRANSACTIONS OF THE ROYAL SOCIETY A MATHEMATICAL, PHYSICAL & ENGINEERING SCIENCES

Tatsumoto, M., Knight, R. J. & Allègre, C. J. 1973 *Science, N.Y.* **180**, 1279–1283.
Treuil, M. 1973 Doctoral thesis, Université d'Orléans.
Treuil, M. & Joron, J.-L. 1975 *Soc. ital. Mineral. Petrol.* **31**, 125–174.
Treuil, M. & Varet, J. 1973 *Bull. Soc. géol. Fr.* (7) **15**, 506–540.
White, W. M. & Schilling, J. G. 1978 *Geochim. cosmochim. Acta* **42**, 1501–1516.
Wood, D. A., Tarney, J., Varet, J., Saunders, A. D., Bougault, H., Joron, J. L., Treuil, M. & Cann, J. R. 1979 *Earth planet. Sci. Lett.* **42**, 77–97.
Zielinsky, R. A. & Frey, F. A. 1970 *Contr. Miner. Petr.* **29**, 242.
Zindler, A., Brooks, C., Arndt, N. T. & Hart, S. R. 1978 *U.S. geol. Surv. Open-File Rep.* no. 701, pp. 469–471.

PHILOSOPHICAL TRANSACTIONS OF THE ROYAL SOCIETY A MATHEMATICAL, PHYSICAL & ENGINEERING SCIENCES